Copy No.

GENERAL DYNAMICS
General Atomic Division

SPECIAL NUCLEAR EFFECTS LABORATORY

P.O. BOX 608, SAN DIEGO, CALIFORNIA 92112

GA-8016

RADIATION EFFECTS ON SILICON

SUMMARY REPORT

November 1, 1965 through April 20, 1967

by

J. A. Naber

H. Horiye

E. G. Wikner

National Aeronautics and Space Administration
Goddard Space Flight System
Contract NAS7-289
GA Project 430

June 20, 1967

ABSTRACT

Research on the radiation-induced displacement effects in silicon included excess minority-carrier lifetime and electron spin resonance measurements. The displacement effects in the silicon were produced by 30-MeV electrons at room temperature; both low-resistivity and high-resistivity (ultrapure) n- and p-type silicon were investigated.

The defects introduced in the high-purity n- and p-type silicon were found to be very near the center of the energy gap and possibly intrinsic defects. The characteristics of these defects were determined by the excess minority-carrier lifetime as measured by the microwave-reflection technique. In the low-resistivity silicon, the defects in the Czochralski-grown (QC) silicon were oxygen-dependent, whereas the defects in the vacuum pulled (FZ) silicon were impurity-dependent. The defects in this low-resistivity silicon were investigated by dc conductivity measurements.

The ESR measurements yielded information about divacancy production, the position of the divacancy energy levels in the energy gap, and Si-G8 formation. However, complete correlation between ESR-detected centers and carrier lifetime recombination levels was not obtained.

CONTENTS

Figures

Figures (continued)

Figures (continued)

I. INTRODUCTION

The purpose of this research program is to study the radiation-induced degradation of lifetime in n- and p-type silicon. The goal of the program is to identify the responsible defects, i.e., whether the defects are intrinsic or are associated with impurities.

A knowledge of the radiation-induced defects that cause lifetime degradation could be used to predict the response of silicon solar cells exposed to space radiation and to recommend changes to minimize such radiation-induced effects. Space radiation consists of low-energy electrons (of a few MeV) and high-energy protons (1 to 100 MeV). As the protons produce the greatest damage, 30-MeV electrons were used to simulate proton damage since they produce a similar type of damage.

To study the defects induced by such irradiation in silicon, measurements of carrier lifetime and electron spin resonance (ESR) were made. Two techniques were used for measuring lifetime. The microwave conductivity technique was used on high-purity silicon and the dc conductivity technique was used on lower resistivity n- and p-type silicon. Temperature dependence of postirradiation lifetime was studied in an attempt to identify recombination levels and pertinent lifetime capture cross section. The ESR technique was used to study defects in irradiated silicon which might be correlated with certain centers seen in the lifetime studies.

II. THEORY OF CARRIER RECOMBINATION AND TRAPPING

The defects produced by atomic displacements introduce energy levels in the forbidden gap of a semiconductor. The energy levels can serve as recombination centers for electrons and holes. The capture of the minority carrier (i.e., holes in n-type material) is generally the rate-limiting step in the recombination process, since the number of majority carriers is much larger than the minority carriers. The excess-carrier lifetime in semiconductors has been investigated from both the experimental and theoretical point of view.[1-5] In principle, the lifetime can reflect the position of the energy level of the capture site in the forbidden gap, so that measurement of the temperature dependence of the lifetime should lead to identification of the defect energy levels.

Present-day theoretical studies of the recombination process in semiconductors are primarily based on the work of Hall[6] and Shockley-Read.[5] The Shockley-Read recombination theory deals with recombination via a single species of recombination center under equilibrium recombination conditions. Under these conditions, the expression obtained for the lifetime, τ, is

$$\tau = \tau_{p_0}\left[\frac{n_0 + n_1 + \Delta n}{n_0 + p_0 + \Delta n}\right] + \tau_{n_0}\left[\frac{p_0 + p_1 + \Delta p}{n_0 + p_0 + \Delta n}\right],$$

where n_0 and p_0 are thermal equilibrium electron and hole concentrations, n_1 and p_1 are the electron and hole concentrations when the Fermi level lies at the recombination center ($n_1 = N_c\, e^{E_R - E_c}/kT$; $p_1 = N_v\, e^{E_v - E_R}/kT$), Δn and Δp are the excess electron and hole concentrations, τ_{n_0} is the electron lifetime governed by the single level when the Fermi level lies close

to the valence band, and τ_{p_0} is the hole lifetime when the Fermi level lies near the conduction band. The excess-carrier recombination lifetime in n-type material can be described by

$$\tau = \frac{-\Delta n}{dn/dt} = \frac{-\Delta p}{dp/dt} = \frac{\tau_{p_0}\left(1 + \frac{n_1}{n_0}\right) + \tau_{n_0}\frac{p_1}{n_0} + \frac{\Delta n}{n_0}\left(\tau_{p_0} + \tau_{n_0}\right)}{1 + \frac{\Delta n}{n_0}} .$$

The excess-carrier lifetime equation can be written as

$$\tau = \frac{\tau_\ell + \tau_h \frac{\Delta n}{n_0}}{\left(1 + \frac{\Delta n}{n_0}\right)} ,$$

where τ_ℓ, the low-injection-level lifetime, is

$$\tau_\ell = \tau_{p_0}\left(1 + \frac{n_1}{n_0}\right) + \tau_{n_0}\frac{p_1}{n_0}$$

and τ_h, the high-injection-level lifetime, is

$$\tau_h = \tau_{p_0} + \tau_{n_0} = \frac{1}{N_R v_{th} \sigma_p} + \frac{1}{N_R v_{th} \sigma_n}$$

in which N_R is the number of recombination centers, v_{th} is thermal velocity of the carriers, and σ_n and σ_p are recombination capture cross sections for electrons and holes. At low injection levels ($\Delta n \ll n_0$), $\tau = \tau_\ell$; at high injection levels, $\tau = \tau_h$.

The parameter measured experimentally is the electrical conductivity. The excess-carrier lifetime is determined from the slope of a semilogarithmic plot of the excess electrical conductivity versus time; the quantity $\Delta n/n_0$ is obtained from the corresponding values of $\Delta\sigma/\sigma_0$ if the mobility is assumed to be constant during the decay. Thus, a linear plot of $\tau(1 + \Delta n/n_0)$ versus $\Delta n/n_0$ yields τ_ℓ from the intercept and τ_h from the slope.

Linearity in this plot is a test of the validity of the single-level recombination assumption. The temperature dependence of τ_ℓ is found in the terms containing τ_{p_0}, τ_{n_0}, n_1, p_1, and n_0, whereas the temperature dependence of τ_h is found in the terms containing τ_{n_0} and τ_{p_0}.

The temperature dependence of τ_{n_0} and τ_{p_0} is exhibited through the thermal velocity, v_{th}, of the carriers and the capture cross section, σ, of the recombination center for the carriers. The temperature dependence of n_1 and p_1 are determined by the position of the recombination center relative to either the valence band or the conduction band, and the temperature dependence of n_0 is determined by the position of the Fermi level relative to the conduction band.

Similar expressions can be obtained for p-type material by interchanging the n's and p's.

Theoretical work on the nature of the temperature dependence of the cross section for neutral and attractive recombination centers has been performed by Lax.[4] The theory of Lax assumes that a carrier is captured into an excited state of large radius followed by a cascade of one-phonon transitions. This initial capturing event is likely to involve an optical phonon or an intervalley collision in the room-temperature range, but the acoustic phonons mainly contribute at low temperatures. Subsequent collisions may eject the electron or cause it to increase its binding energy. The "sticking probability," or the probability of eventual capture into the ground state, becomes significant for binding energies of order kT. As the temperature is reduced, capture into orbits of larger radius becomes effective. The optical processes are most important in the 70°K to 400°K range.

Lax's calculation for the attractive cross section for the optical processes gives

$$\sigma_{(opt)}(T) = \sigma_0 \lambda \left[1 - \exp(-\lambda)\right]^{-1} D(\lambda) ;$$

the functions $D(\lambda)$ and $\lambda = \hbar\omega/kT$ are defined and tabulated in Ref. 4. For a singly charged center ($Z = 1$), $\sigma_0 = 10^{-14}$ cm^2.

The calculation for electron capture by a neutral center has also been given. Lax assumes a polarization potential of the form $V \propto 1/r^4$ for which no stationary closed orbits exist. The electron will spiral inward, and it is assumed that the sticking probability is essentially unity. The formula for the neutral-interaction cross section is:

$$\sigma = 1.7 \times 10^{-15} \lambda[1 - \exp(-\lambda)]^{-1} \text{ cm}^2 ,$$

for which the temperature dependence is nearly $1/T$ for the temperature range of interest.

The distinction between a recombination center and a trap is quantitative rather than a qualitative one. A minority carrier is captured at a center. If the carrier lives a mean lifetime in the captured state and is ejected (e.g., thermally), we may regard the center as a trap. If, however, a majority carrier is trapped before thermal ejection can occur, recombination will have taken place and the center may be regarded as a recombination center. Which role a center will play depends, then, on the concentration of majority carriers and on the relative cross sections for capture of minority and majority carriers. Extensive treatment of trapping can be found in papers by Baicher,[3] Streetman,[7] and Nomura and Blakemore.[8,9]

III. MICROWAVE-REFLECTION MEASUREMENTS

3.1. INTRODUCTION

The nature of lattice defects, which are produced by irradiation of silicon, has been the subject of a considerable amount of experimental study. Experimental investigations have included measurement of changes in resistivity, Hall coefficient, infrared absorption, photoconductivity, electron spin resonance (ESR), and excess-carrier lifetime. The excess-carrier lifetime is a highly sensitive indicator of radiation damage in semiconductors. The dependence of the lifetime on sample temperature and concentration of excess carriers can be used to determine both the energy level and the relative electron and hole capture cross sections of the dominant recombination center. Additional information about the nature of the radiation-induced defect can be obtained from isothermal and isochronal annealing studies. In general, the study of radiation effects in silicon at cryogenic temperatures (using electrical measurements taken at a temperature as low as 4.2°K) has always been hindered by an uncertainty in the quality of the electrical contacts on the silicon sample. Ohmic contacts on silicon, which are effective at cryogenic temperatures, are almost impossible to apply with current technology.[10] The microwave reflection technique of measuring the excess-carrier lifetime circumvents this contact problem.

The objective of the microwave reflection program discussed here is to study the defects introduced in high-purity n- and p-type silicon by 30-MeV electrons. The defects introduced in each of these materials should be intrinsic defects; i.e., they are not dependent on doping or crystal-growth techniques. The measurements were carried out principally at room-temperature irradiations since this research is directly related to the study of defects introduced at comparable temperatures in silicon solar cells in space vehicles. However, one group of measurements was made at liquid-helium temperature.

3.2. EXPERIMENTAL TECHNIQUES

3.2.1. General Theory

During the initial portion of this contract period, steps were taken to correct inadequacies that existed in the microwave-reflection measuring bridge. These changes only slightly altered the method previously employed[2] to measure the transient and quiescent electrical conductivity of semiconductors.

The basic principles involved in impinging a plane microwave in a waveguide on a slab of semiconductor material placed against the end of a waveguide have not changed. The complex propagation constant of the microwave in the semiconductor materials can be deduced by observing the amplitude of the reflected microwave signal.

The microwave propagation system shown schematically in Fig. 1 was used for the experiments reported here. Microwave power of 8.7 Gc is generated by a klystron oscillator, and a ferrite isolator is utilized to minimize perturbations on the klystron due to microwave reflections downstream. The variable attenuator determines the amplitude of the microwave signal to be used for the experiment. The 20-db directional coupler selects a small fraction of the microwave power and transmits it to a calibrated adjustable cavity. The cavity is set to resonate at 8.7 Gc, and at this frequency crystal detector 1 exhibits a minimum reflected amplitude. The cavity and crystal detector 1 are utilized to stabilize the oscillator frequency. The frequency of the klystron is stabilized by the use of an automatic frequency control. Looking at the signal from the reference cavity, which acts as a discriminator, one obtains an amplitude-modulated signal whose phase depends on whether the klystron frequency is above or below the frequency of the referenced cavity. This signal is then phase-sensitive detected, thus providing a dc voltage that is fed back to the klystron reflector for stabilization. This arrangement is required because

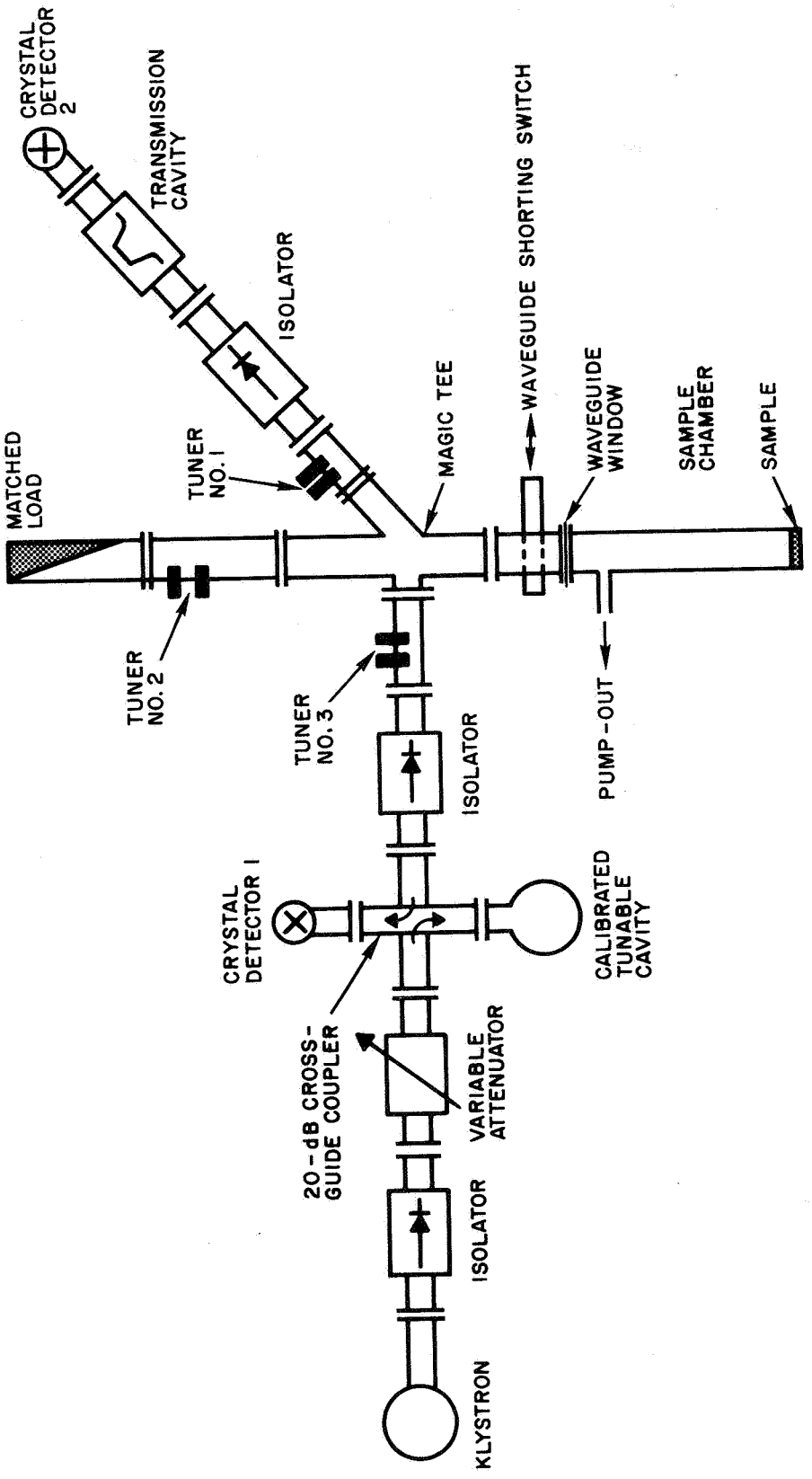

Fig. 1--Microwave system

the signal reflected from the semiconductor sample is a function of frequency and the calibration of transmission cavities used elsewhere in the microwave circuit varies with changing frequency.

Behind the directional coupler, another ferrite isolator is used to minimize interactions between components of the microwave circuit. The microwave signal generated then impinges on a "Magic Tee," which divides the power equally between two arms. One-half of the power is discarded in the matched load in one arm and one-half passes to the sample located at the shorted end of a thin-wall stainless-steel waveguide.

The signal reflected from the sample arm is transmitted back to the Magic Tee, where one-half of it is transmitted to a monitoring arm consisting of a ferrite isolator, transmission cavity, and crystal detector 2. The transmission cavity in front of crystal detector 2 is required because the linear accelerator beam used to produce ionization in the sample is modulated at L-band frequencies and a harmonic of this frequency can be propagated down the waveguide and detected in the crystal. These harmonics are rejected by utilizing transmission cavities tuned to the klystron frequency. Furthermore, the klystron frequency has been carefully chosen to lie almost midway between the harmonics of the accelerator operating frequency. The ferrite isolator is again utilized to keep signals reflected from the transmission cavity and crystal from being reflected into other sections of the experimental equipment. Crystal detector 2 monitors both the amplitude of the reflected signal and the signal incident on the semiconductor sample. The incident signal is measured by shorting the line across the sample chamber with a waveguide switch. The ratio of these two microwave powers can then be employed to calculate the power absorbed in the sample and thus its conductivity.

To reduce spurious reflected signals and cross coupling, three tuners are included in the microwave circuit. These tuners consist of two screws (provided with lock nuts) that penetrate the center of the broad

face of the length of waveguide and are separated one-fourth of a guide wavelength at the operating frequency. By adjusting the penetration of these two screws and by moving the tuner forward or backward one-fourth of a wavelength with respect to the reflection being tuned out, it is possible to cancel any spurious reflected signals.

The sample is mounted in the end of the waveguide, as shown in Fig. 2. The sample is soldered onto the copper short, which is soldered onto the bottom end of the waveguide; this seal is vacuum tight. The waveguide is evacuated through an 0.008-in.-wide slot cut in the broad face of the waveguide just below the upper flange and pressure window. A piece of 2-mil Mylar is used as the waveguide vacuum window. This window produces no measurable attenuation of the microwave energy.

The temperature sensors, a copper-constantan thermocouple and a 47-ohm, 0.1-W carbon-composition resistor, are attached to the bottom of the copper short. With this arrangement, temperatures between 4.2°K and room temperature are easily measured. Two glass vacuum dewars are placed around the waveguide when liquid-helium and liquid-nitrogen temperatures are desired. The outer dewar is always filled with liquid nitrogen and the inner dewar is filled with liquid helium or liquid nitrogen, depending on the sample temperatures desired. Temperatures above those of the liquid coolants are obtained by expelling the coolant by adding small pulses of room-temperature gas (helium) into the working space at the top of the sample holder. This working space is enclosed with a top plate through which passes the waveguide, electrical feedthroughs, and fill and vent lines. The gas enclosed in the dewar acts as a thermal reservoir, which provides adequate thermal stability for several minutes between stepwise temperature increases.

The calibration of the signal from crystal detector 2, in terms of power, is accomplished by removing the sample chamber from the microwave circuit and replacing it with a power meter. The variable attenuator is

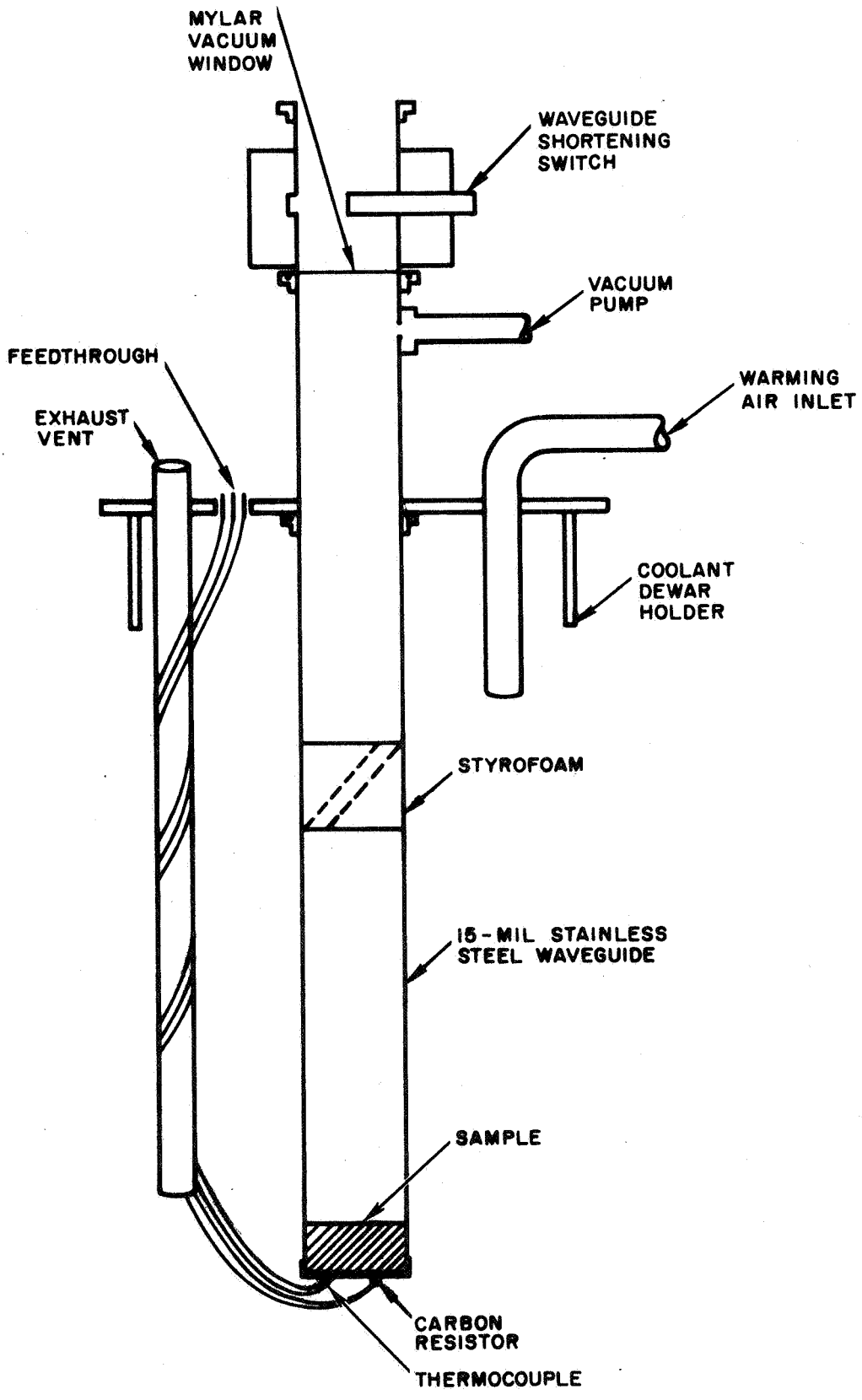

Fig. 2--Sample-holder configuration

varied and the signal at crystal detector 2 is related to the reflected power.

The data-analysis procedures for measuring the change in conductivity for a particular semiconductor sample are as follows:

1. The changes in voltage from the microwave crystal detector 2 are measured with the radiation-effects amplifier and oscilloscope recording system. The incident and reflected quiescent voltages are recorded on chart recorders.

2. These voltages are related through crystal detector 2 calibration to the microwave power incident and reflected from the sample.

3. The absorption coefficient of the sample is calculated by taking the ratio of the microwave powers.

4. A calibration curve for a given set of sample dimensions and dielectric constant is used to evaluate the electrical conductivity from the absorption coefficient. This calibration curve is computed from the theory presented in Ref. 2.

5. The time dependence of the conductivity is plotted (by a computer) and fitted to an exponential decay curve.

The above procedure is carried out by computer programming and semiautomatic data processing.

3.2.2. Limitations

The microwave-reflection technique for measuring transient and quiescent electrical conductivity has certain limitations which must be satisfied before successful experiments can be performed.

In the microwave-reflection experiments only the amplitude of the reflected microwave signal is measured. This makes it necessary to assume that the dielectric constant (K) does not change during the course

of either the transient or quiescent electrical conductivity measurements. Using a value of 11.7 for the carrier-free dielectric constant (K_0) for silicon and a fixed sample thickness, the logarithm of the ratio of incident to reflected signal versus electrical conductivity shown in Fig. 3 was calculated using the computer program.

The dielectric constant (real part) is composed of two parts

$$K = K_0 + \Delta K ,$$

where ΔK, the carrier contribution[11] to the dielectric constant, is

$$\Delta K = - \frac{4\pi\sigma_0\tau}{1 + (\omega\tau)^2} ,$$

in which σ_0 is the dc electrical conductivity, τ is the relaxation time, and ω is the microwave angular frequency. For n- and p-type silicon and for the frequency and temperature range used, $\omega\tau \ll 1$;[12] therefore,

$$\Delta K = - \frac{4\pi}{e} \sigma_0 \mu_H m^* ,$$

where μ_H is the Hall mobility and m* is the effective mass of carriers. For $\sigma_0 < 0.1$ (ohm-cm)$^{-1}$, the variation of ΔK is insignificant compared with K_0.[13]

Therefore, for the injection levels and temperature ranges used in these experiments, it is a good approximation to assume that the dielectric constant is constant.

In a like manner, the electrical conductivity is dependent on the carrier relaxation time and on the angular frequency of measurement[11] by

$$\sigma = \frac{\sigma_0}{1 + (\omega\tau)^2} .$$

For the frequency and temperature range for n- and p-type silicon, $\omega\tau \ll 1$[12] and thus the dc electrical conductivity is measured.

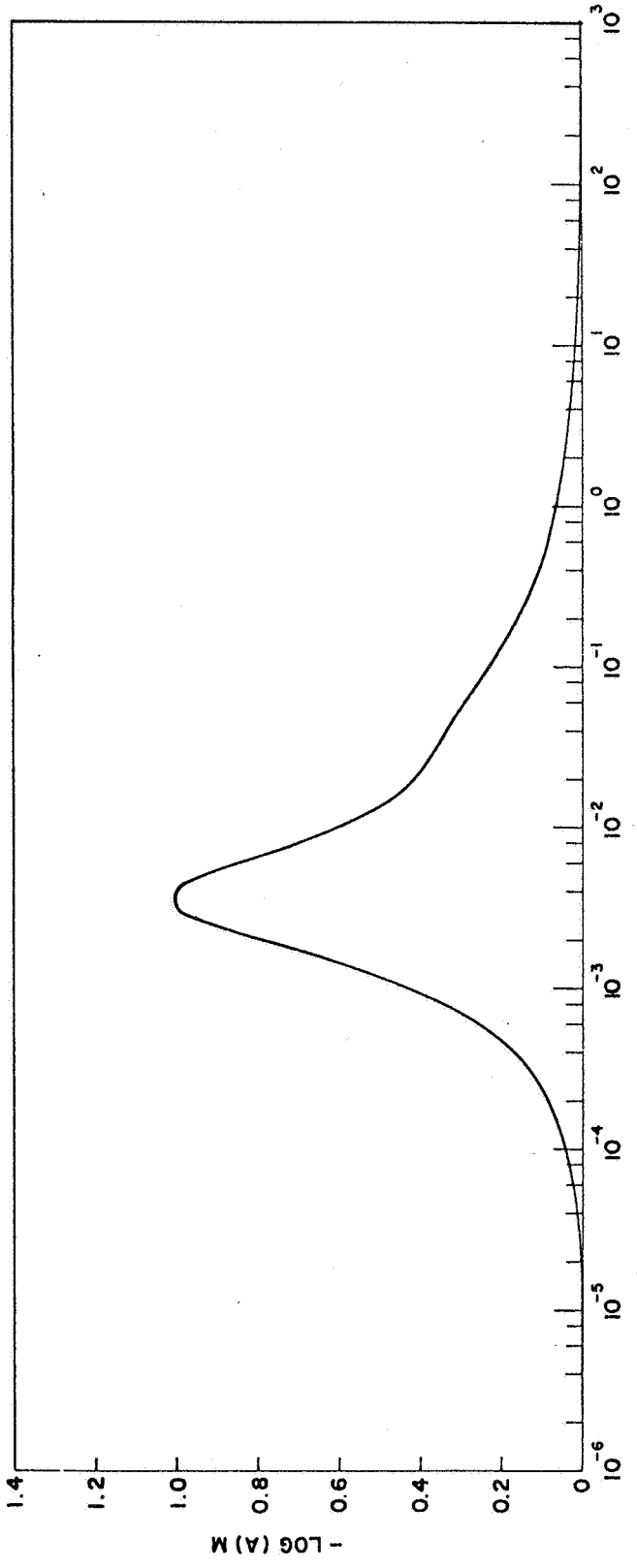

Fig. 3--Ratio of incident power to reflected power as a function of electrical conductivity for a dielectric constant of 11.7 and sample thickness of 1.3228 cm

A final limitation on the microwave-reflection measurements is the contact between the semiconductor and the waveguide walls. In theory, it is assumed that there is perfect contact. However, when the semiconductor is cut and lapped to fit into the waveguide, the contact is not perfect. Work published by Champlin[14] has shown that for the low-conductivity samples used in these experiments, the effect of imperfect fit can be neglected.

3.2.3. Sample Preparation

The n- and p-type, single-crystal, high-resistivity ($> 10^4$ ohm-cm) samples were all prepared alike. The samples were cut from boules of silicon by a diamond saw to the approximate dimensions of 0.900 in. by 0.400 in. by $\sim$ 0.500 in. The samples were lapped on 600 carborundum paper to fit snugly into the waveguide. The base of the sample was then nickel-plated (electrodeless)[15] and then tinned with 60-40 solder. The sample was then soldered onto the copper short at the end of the waveguide. The sample was orientated so that the electron beam would strike the sample in the $\langle 110 \rangle$ direction.

The electron beam was 0.1-μsec pulses of 100-mA 30-MeV electrons. The electron fluence was administered to the sample in single pulses with a repetition rate of about 2 per second. The sample was 10 in. from the beam exit and the beam was scattered by a 3/16-in. aluminum scatterer. The electron fluence was determined by the calibration of a thermistor in conjunction with a secondary emission foil.

The electron linear accelerator (Linac) and flash x ray (200 KVp x-ray pulse 0.1 μsec wide) were used to inject the excess carriers into the semiconductors, and scatterers were placed between the beam port and the sample to vary the injection level. Whenever measurements were made using the microwave bridge, the sample chamber was evacuated to at least 1 μ Hg pressure or better. Measurements were made over a range from 4.2°K to 475°K.

The materials used in these experiments were specially purchased. The n-type silicon was purchased from Wacker Chemical Company of Germany. It was doped with phosphorous and was vacuum floating-zone grown with an etch-pit count of 1.3×10^4 cm^{-2}. Its room-temperature excess-carrier lifetime was 1000 μsec. The p-type silicon was obtained from Shin-Etsu Chemical Industry Company of Japan. It had a low oxygen content and its initial lifetime was 1100 μsec.

3.3. EXPERIMENTAL RESULTS

3.3.1. n-type Silicon

3.3.1.1. Unirradiated Sample. Transient and quiescent electrical conductivity measurements of the silicon samples used in these experiments were first performed on the unirradiated material. These measurements were performed at the flash x-ray facility in a temperature range from liquid-nitrogen to room temperature. Figure 4 shows the low-injection-level lifetime, τ_ℓ, as a function of 1000/T (°K). There is an injection-level dependence of this excess-carrier lifetime. The ratio of high-level-injection lifetime to low-level-injection lifetime, τ_h/τ_ℓ, is approximately 2 over the whole temperature range. Figure 5 shows the electrical conductivity, σ, as a function of 1000/T (°K). The general characteristics of the shape of the electrical-conductivity curve is in agreement with theory for n-type silicon.[16, 17] The decrease in conductivity in going from 77.5°K to 300°K is caused by increased lattice scattering.

The general technique for obtaining the lifetime data from the microwave-reflection technique is now described. Assuming a constant dielectric constant and a fixed sample thickness, the logarithm of the ratio of the reflected power to incident power as a function of electrical conductivity was plotted (see Fig. 3). A photograph was taken of the oscilloscope trace of the microwave signal voltage from crystal detector 2 (Fig. 6). Using a computer program,[2] the electrical conductivity as a function of

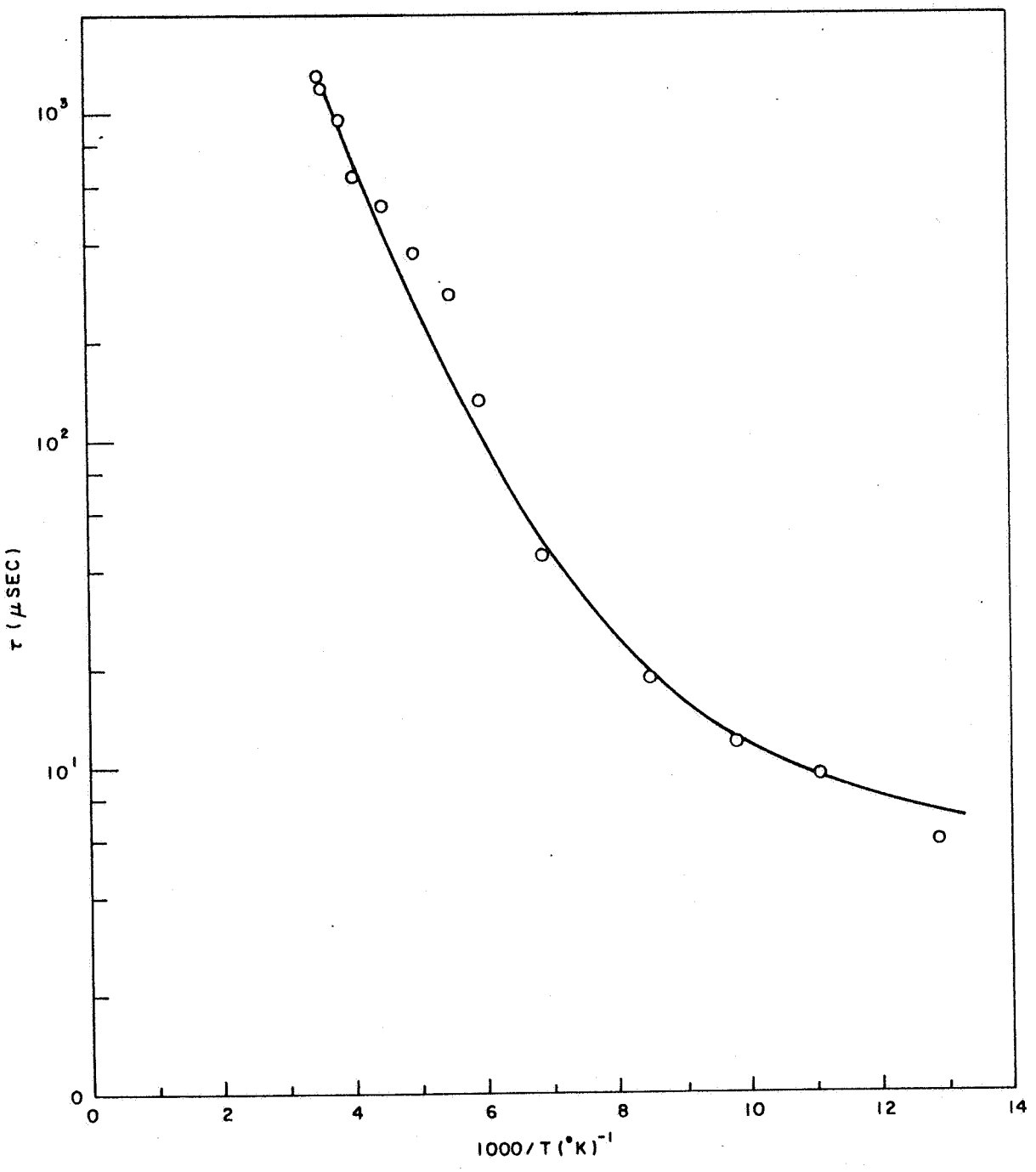

Fig. 4--Inverse temperature dependence of low-level-injection carrier lifetime for n-type silicon

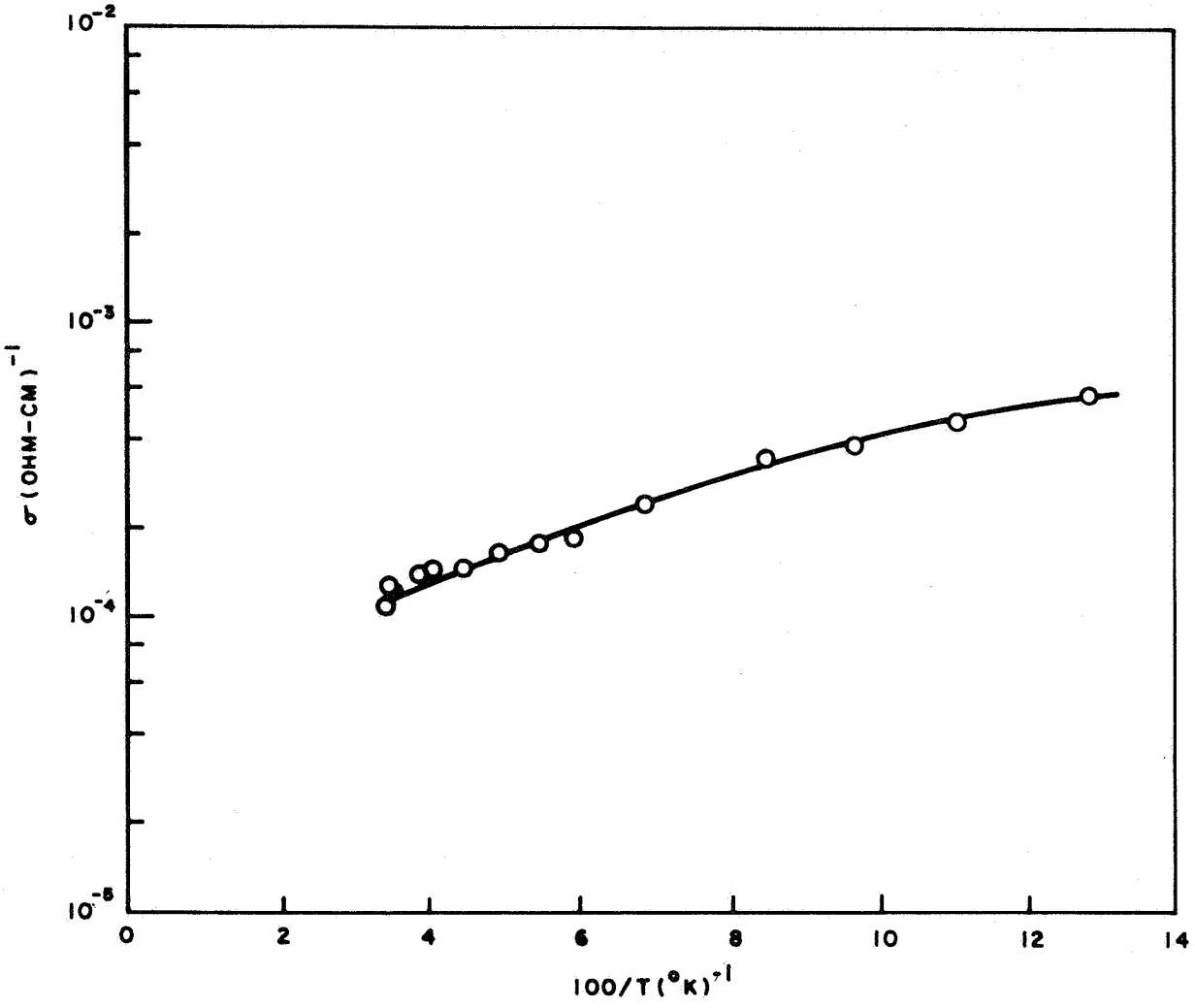

Fig. 5--Preirradiation electrical conductivity as a function of inverse temperature

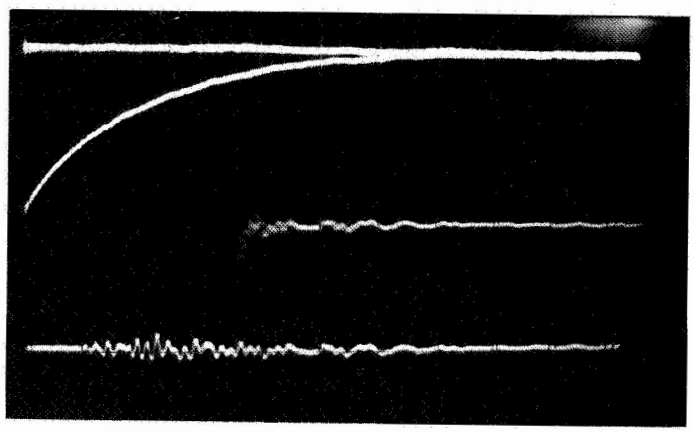

Upper beam: Microwave conductivity signal

Lower beam: Linac beam monitor

Fig. 6--Observed signals for microwave conductivity measurement

time was computed; a typical plot is shown in Fig. 7. The computer program is also used to evaluate

$$\frac{\sigma_f - \sigma_t}{\sigma_f - \sigma_0} = e^{-t/\tau},$$

where σ_0 and σ_f are the initial and final electrical conductivities, respectively, σ_t is the conductivity at any time t, and τ is the lifetime of the excess conductivity. Figure 8 shows a typical computer semilog plot of $\sigma_f - \sigma_t / \sigma_f - \sigma_0$ versus t.

Attempts were made to analyze the lifetime data in the unirradiated n-type silicon sample using the Shockley-Read recombination theory and the temperature dependence of the carrier capture cross section of Lax. The results of this approach did not fit the experimental data because the experimental-data temperature dependence was much more severe than that predicted by theory. Complete analysis of the data was not performed because the recombination properties of the defects introduced by electron irradiation were of primary concern. However, it may be possible to analyze the data in terms of two recombination centers. This approach has been taken by Ivanov.[18]

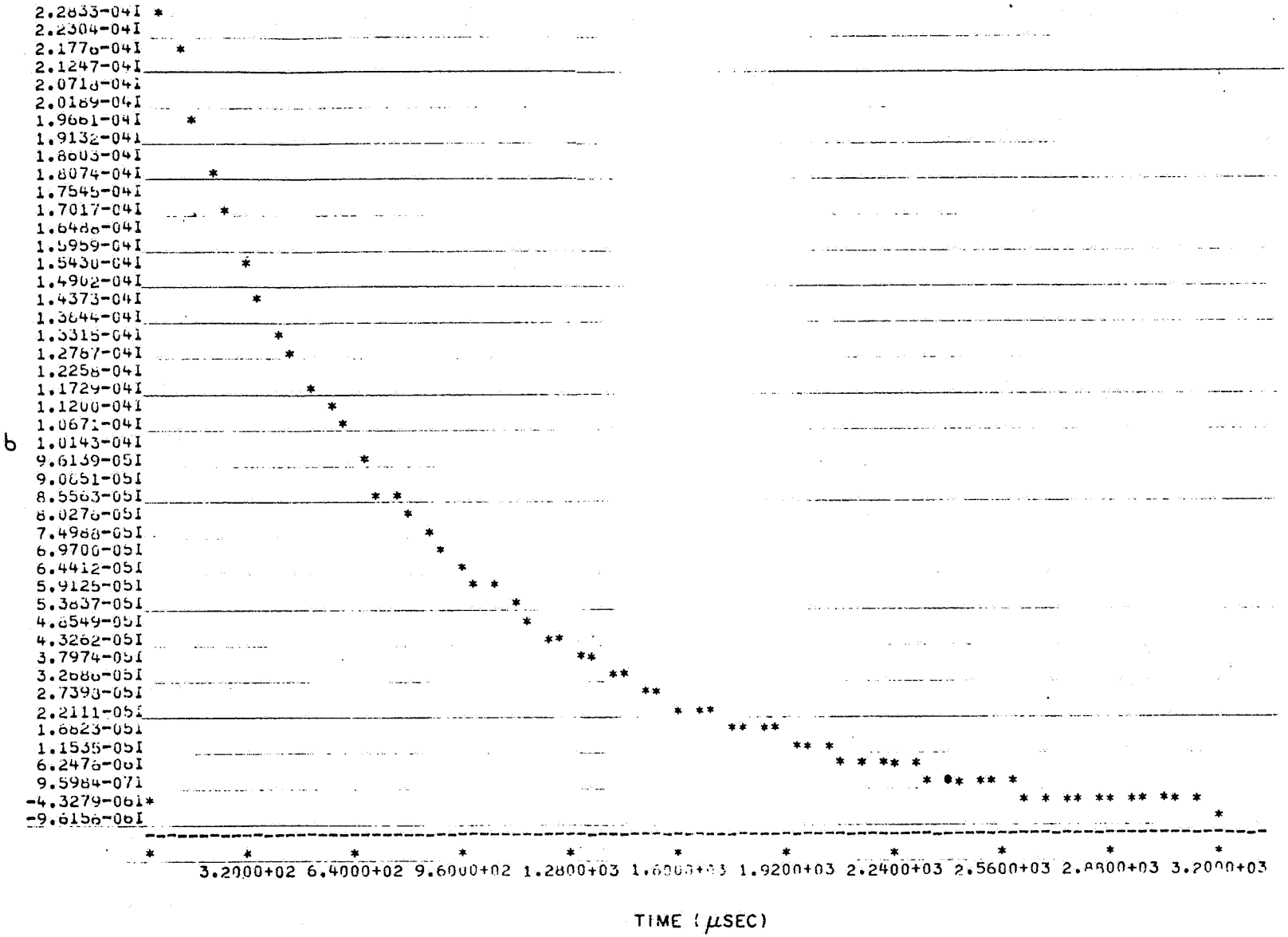

Fig. 7--Electrical conductivity as a function of time after injection of carriers

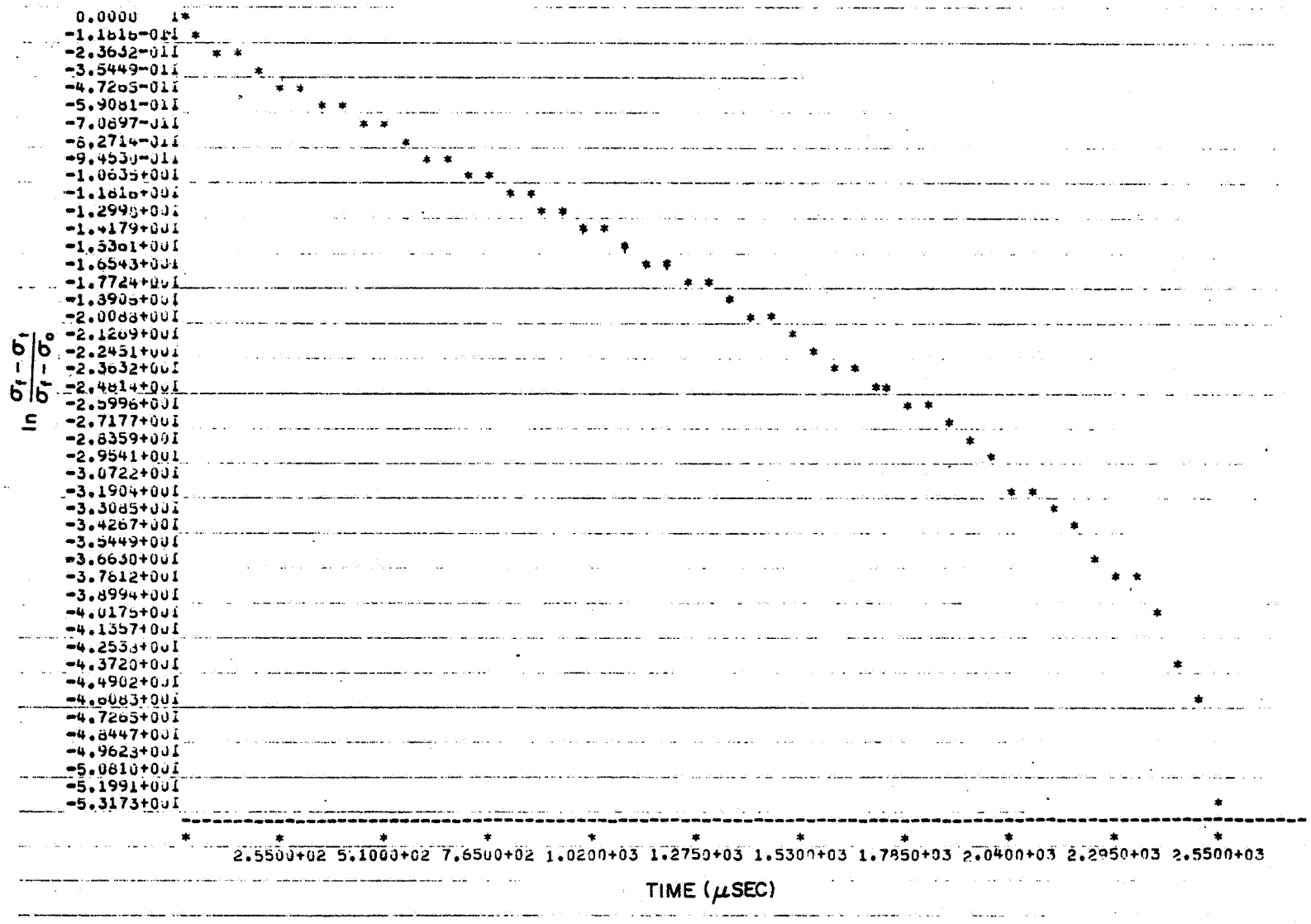

Fig 8 --Logarithmic plot of electrical conductivity as a function of time after injection of carriers

3.3.1.2. 30-MeV Electron Irradiation. Irradiation of the high-purity n-type silicon with 30-MeV electrons at room temperature was performed in two phases. The lifetime was first degraded by a factor of three and then the temperature dependence of the lifetime was measured using the flash x-ray facility for injection. The silicon sample was irradiated again with 30-MeV electrons and the temperature dependence of the lifetime was again measured using the flash x-ray for injection. Figures 9 and 10 show the measurement during the first phase. Figure 9 shows the fluence dependence of the inverse lifetime. This data is plotted according to the relationship

$$\frac{1}{\tau} = \frac{1}{\tau_0} + K\Phi ,$$

where τ is the measured low-injection-level lifetime after a fluence Φ, τ_0 is the initial lifetime at $\Phi = 0$, and K is the lifetime degradation constant. Figure 10 shows the inverse temperature dependence of the low-injection-level carrier lifetime. It should be noted that after the irradiation of 8.2×10^{10} electrons/cm^2, there is a trapping center present at low temperatures.

During the second phase, the lifetime was degraded to 70 μsec by a fluence of 3.94×10^{11} electrons/cm^2. Figure 11 shows the fluence degradation of the lifetime. The degradation constant from Figs. 9 and 11 is $2.0 \pm 0.2 \times 10^{-8}$ cm^2/electron sec. The temperature characteristics of the lifetime (shown in Fig. 12) indicate that a recombination center and a trapping center are still present. It should be noted here that the inverse lifetime degradation was linear throughout the whole flux range and that there was no noticeable room-temperature annealing of the lifetime. The injection-level dependence of the carrier lifetime at room temperature after the second irradiation is shown in Fig. 13. The plot is linear and the ratio of τ_h / τ_ℓ is ~ 1.5. This is no doubt the injection-level dependence

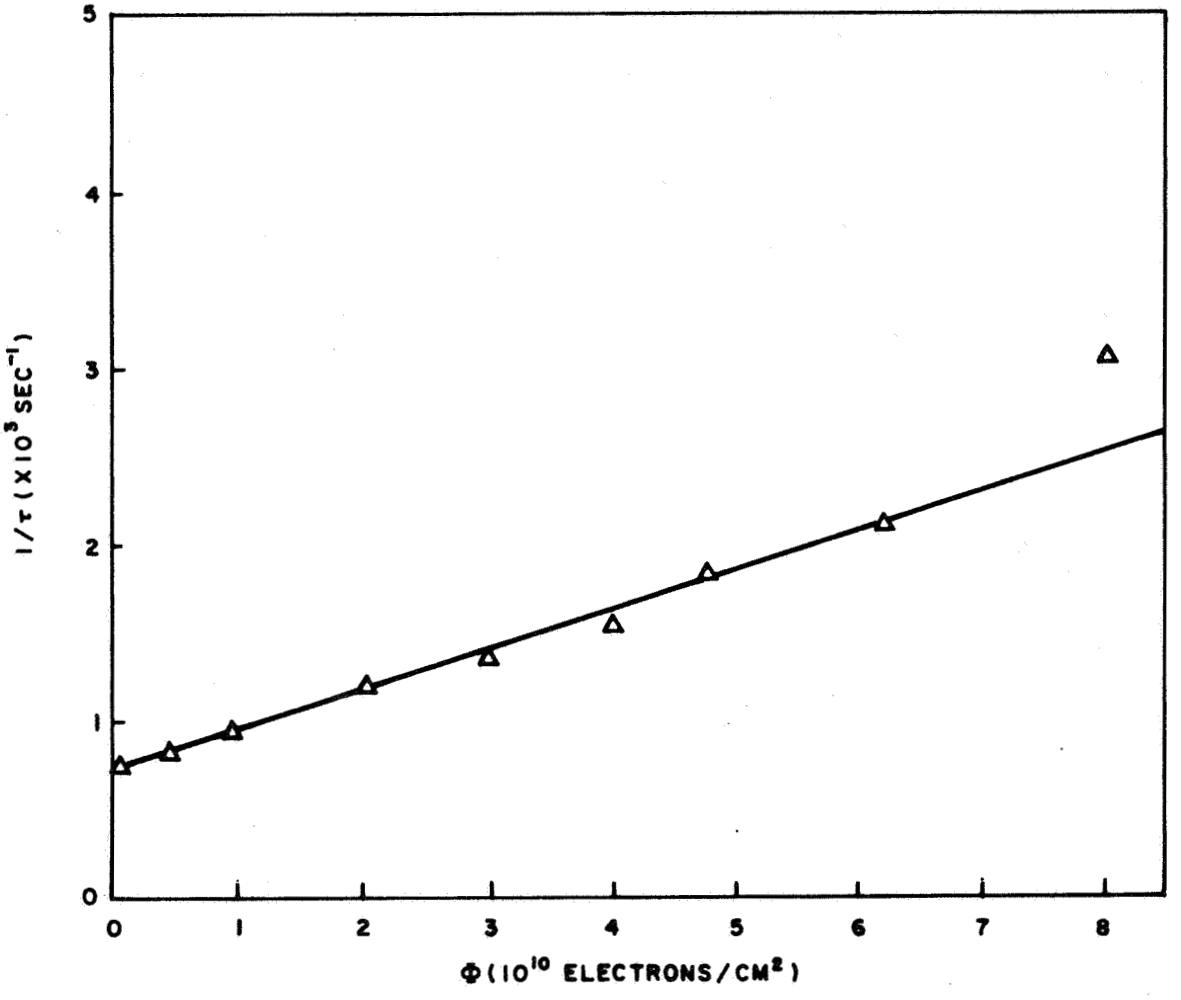

Fig. 9--Inverse lifetime as a function of electron fluence

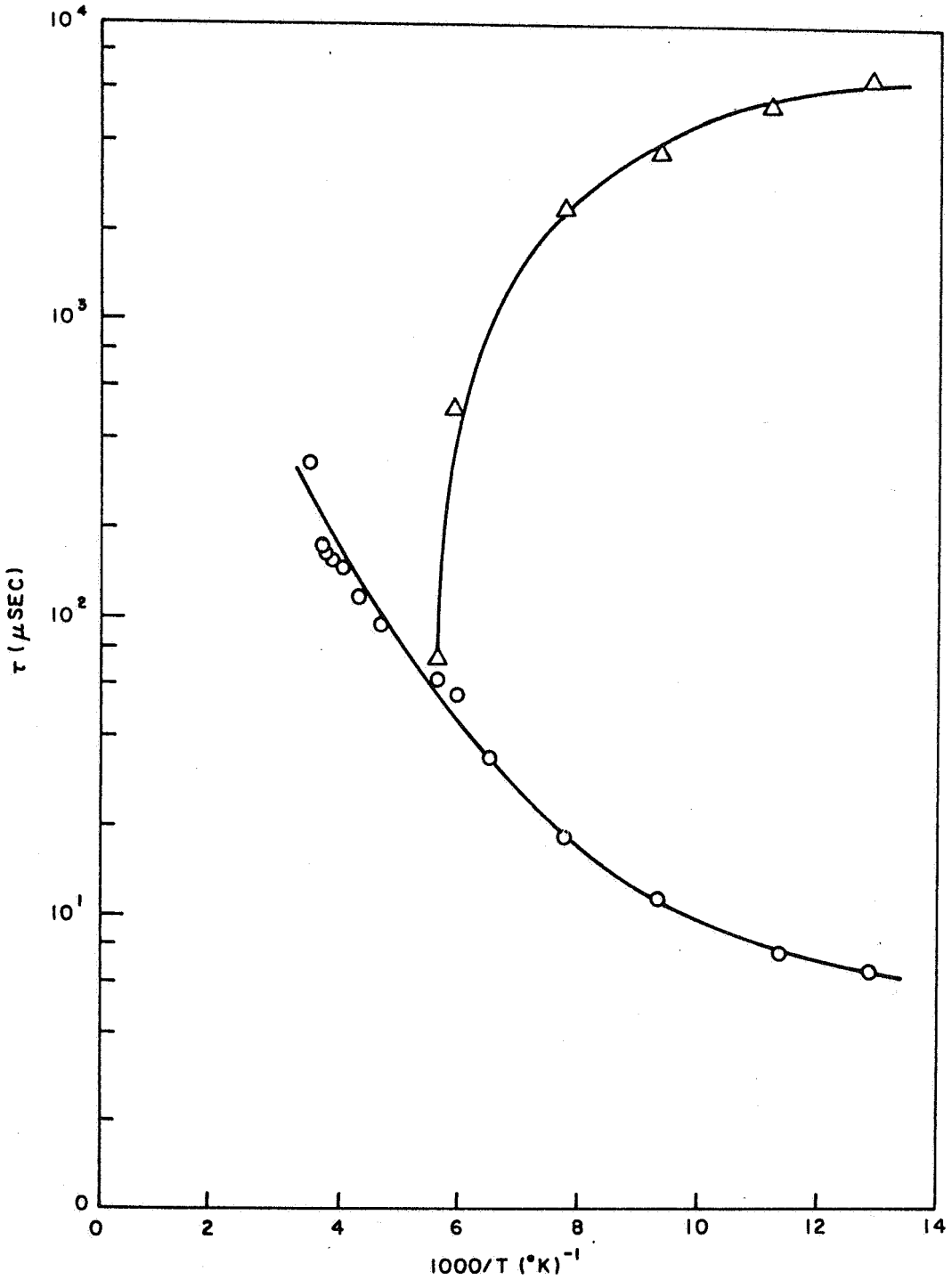

Fig. 10--Carrier lifetime as a function of inverse temperature after Linac irradiation

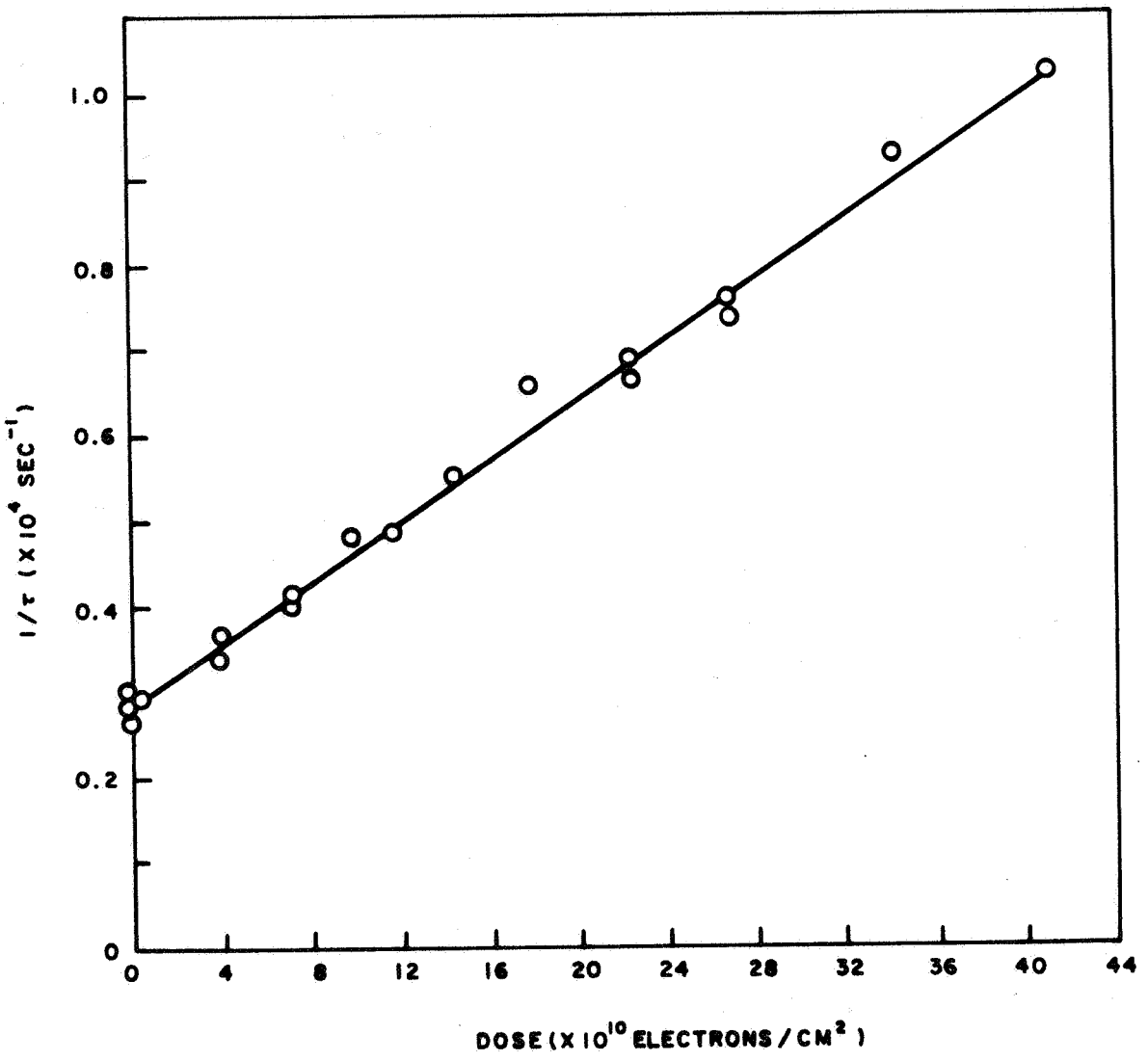

Fig. 11--Degradation of carrier lifetime for n-type silicon at room temperature after 30-MeV electron irradiation

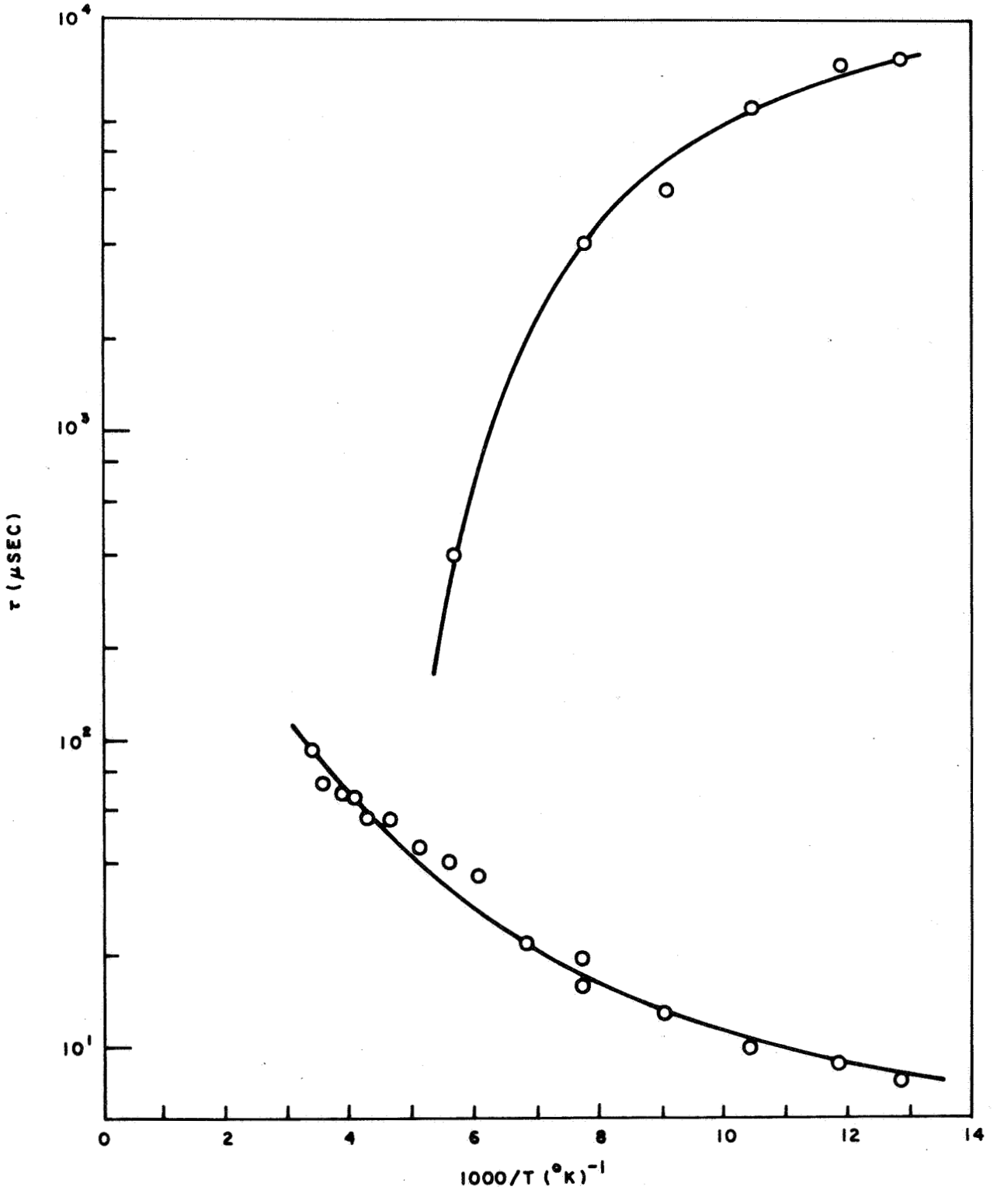

Fig. 12--Temperature dependence of excess-carrier lifetime after irradiation with 30-MeV electrons

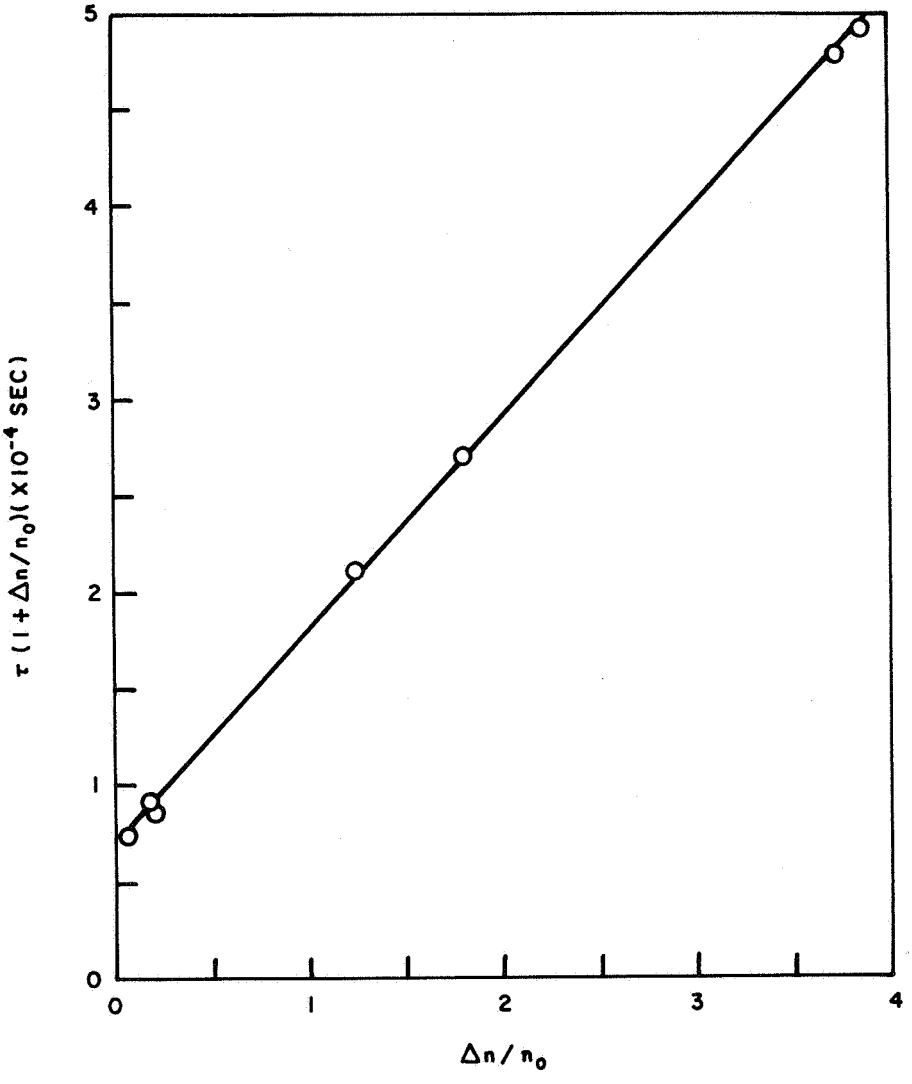

Fig. 13--Injection-level dependence of carrier lifetime for n-type silicon after 30-MeV electron irradiation

of the radiation-induced recombination center, since the lifetime of the virgin material is degraded by at least a factor of 15. The injection-level dependence at liquid-nitrogen temperature is difficult to obtain at this point because the measured lifetime is composed of radiation-induced trapping, radiation-induced recombination, and recombination due to the center present in the virgin material.

The plot in Fig. 14 shows the electrical conductivity as a function of inverse temperature after the second irradiation. It is clear that during the above irradiations, the resistivity of the sample increased at all temperatures.

The damaged sample was annealed isochronally for 20 min at temperatures between room temperature and 475°K. It can be seen from Fig. 15 that the lifetime starts to recover near 360°K and recovers gradually.

3.3.1.3. Irradiation at Liquid-helium Temperature. At liquid-helium temperature, the lifetime (high injection levels) of excess electrical conductivity consists of two very short time constants--one of ~ 0.2 μsec and the other 3 μsec. Measurements during irradiation with 25-MeV electrons show that up to integrated fluxes of 1.1×10^{12} electrons/cm^2, there is no noticeable change in the decay lifetime. Even though there was no observable effect on the properties of the sample irradiated at 4.2°K, considerable changes at liquid-nitrogen temperature were observed. The preirradiation electrical conductivity at liquid-nitrogen temperatures was 8×10^{-4} (ohm-cm)$^{-1}$; after irradiation at 4.2°K, it was $< 2 \times 10^{-5}$ (ohm-cm)$^{-1}$ at liquid-nitrogen temperature. The preirradiation lifetime of excess conductivity at liquid-nitrogen temperature was 20 μsec and the lifetime after the 4.2°K bombardment was 2×10^4 μsec at liquid-nitrogen temperature. The excess-carrier lifetime for the sample after it had been irradiated at 4.2°K and annealed to 340°K is shown in Fig. 16. These decays fit a first-order kinetic process. The inverse temperature dependence of the lifetime indicates that a trapping center is responsible for the decay of the excess conductivity.

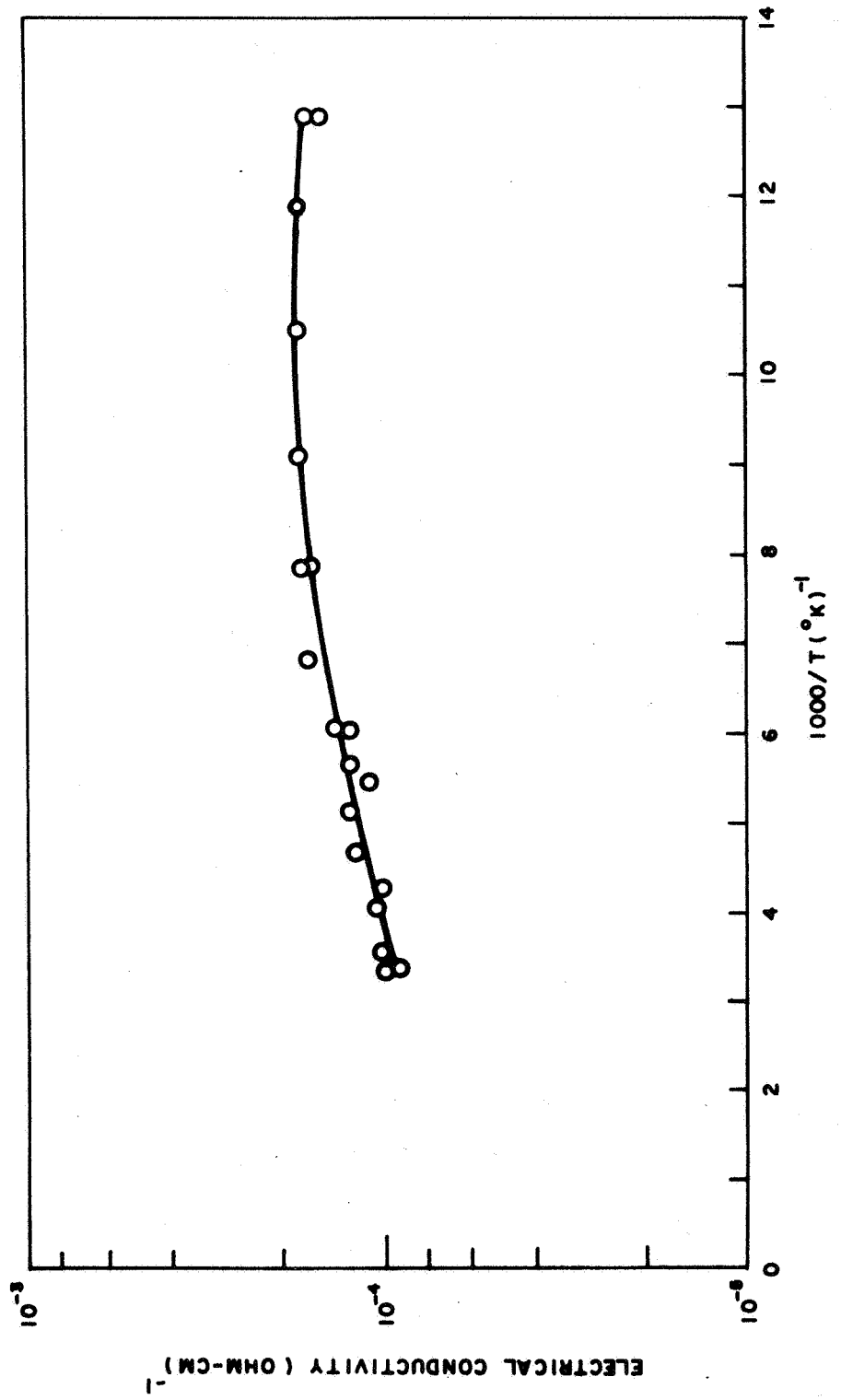

Fig. 14--Temperature dependence of electrical conductivity for n-type silicon after 30-MeV electron irradiation

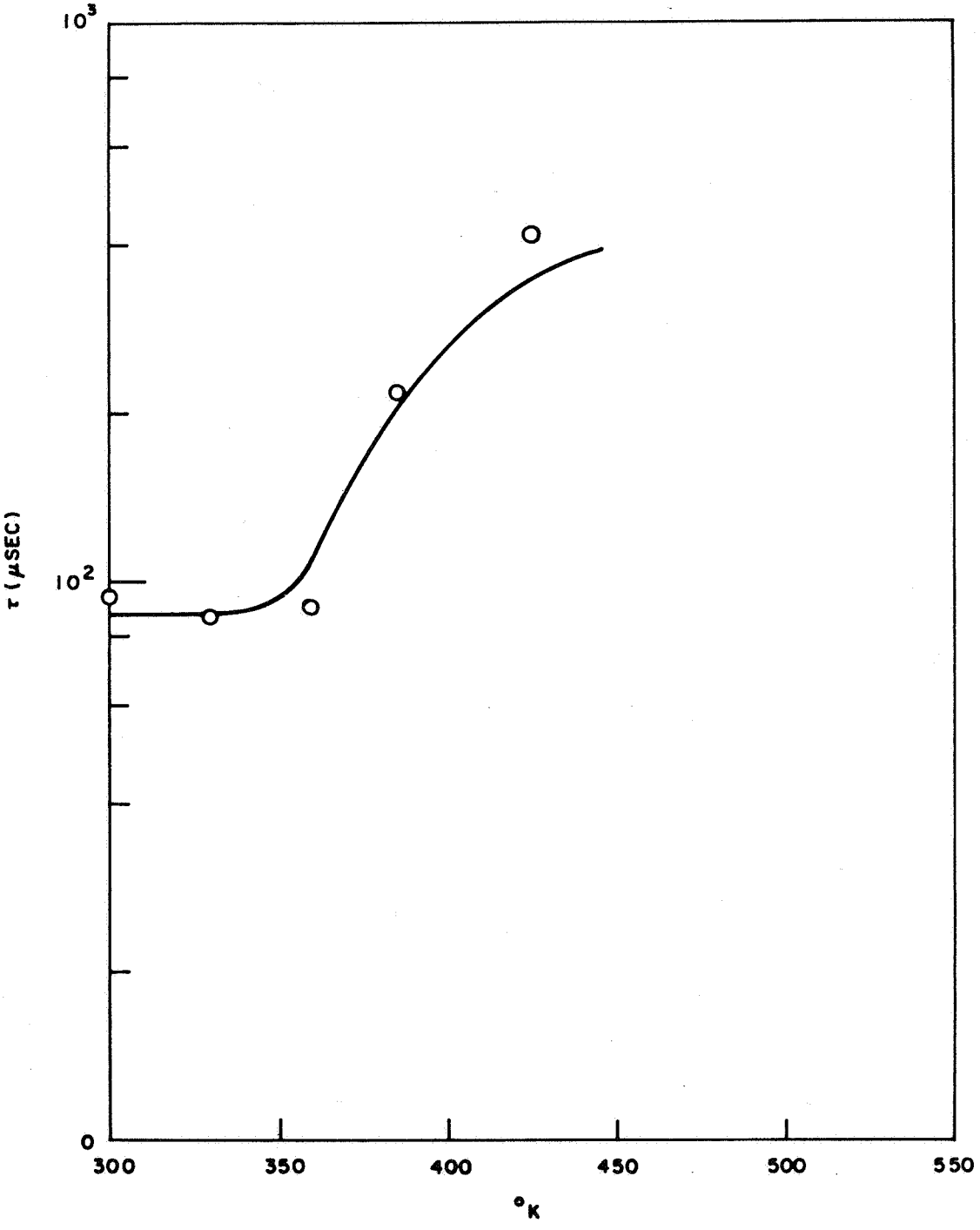

Fig. 15--Isochronal annealing of lifetime of n-type silicon after 30-MeV electron irradiation at room temperature

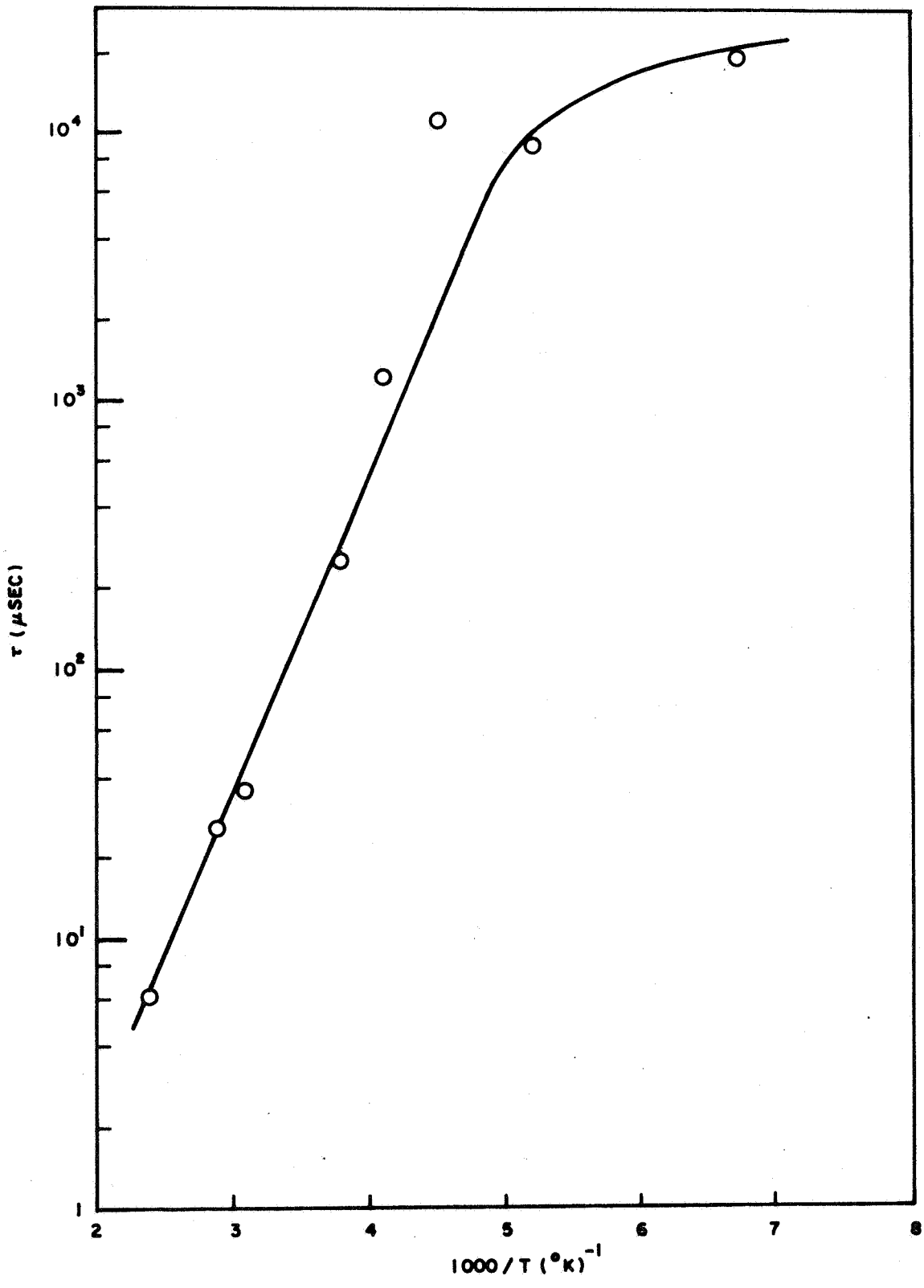

Fig. 16--Inverse temperature dependence of lifetime of high-purity n-type silicon after irradiation at 4.2°K and anneal to 340°K

3.3.2. p-type Silicon

The temperature dependence of the low-injection-level lifetime and electrical conductivity of unirradiated p-type silicon are presented in Figs. 17 and 18. The injection-level dependence for this p-type sample ranges from τ_h/τ_ℓ of ~ 1.5 at room temperature to 5 at liquid-nitrogen temperature. As was the case with the n-type material, it is not possible to explain the temperature dependence of the lifetime by the Shockley-Read and Lax theories. Again, the observed temperature dependence may be due to two recombination centers.

The p-type silicon experiments were performed in two phases in the same manner as the n-type material. The initial 30-MeV electron irradiation at room temperature degraded the inverse low-injection-level lifetime, as shown in Fig. 19. The inverse temperature dependence of the low-injection-level lifetime after this irradiation is shown in Fig. 20. For the second irradiation, the degradation of the lifetime and the temperature dependence of this degraded lifetime are plotted in Figs. 21 and 22. During both irradiations, the lifetime degradation constant is $2.5 \pm 0.3 \times 10^{-8}$ cm^2/electrons sec. It should be noted that the lifetime degradation in Fig. 21 decreases at large fluences. Figure 22 indicates a recombination center and a trapping center. The trapping center was not present after the first irradiation of 1.1×10^{11} electrons/cm^2. The injection-level dependence of the room-temperature lifetime is linear and the τ_h/τ_ℓ ratio is 1.4. The inverse temperature dependence of the electrical conductivity after the second irradiation is presented in Fig. 23. The resistivity of the sample has increased during the fluence of 8.05×10^{11} electrons/cm^2. There is no noticeable annealing of lifetime or electrical conductivity at room temperature.

3.4. INTERPRETATION

The properties of the recombination center introduced in n- and

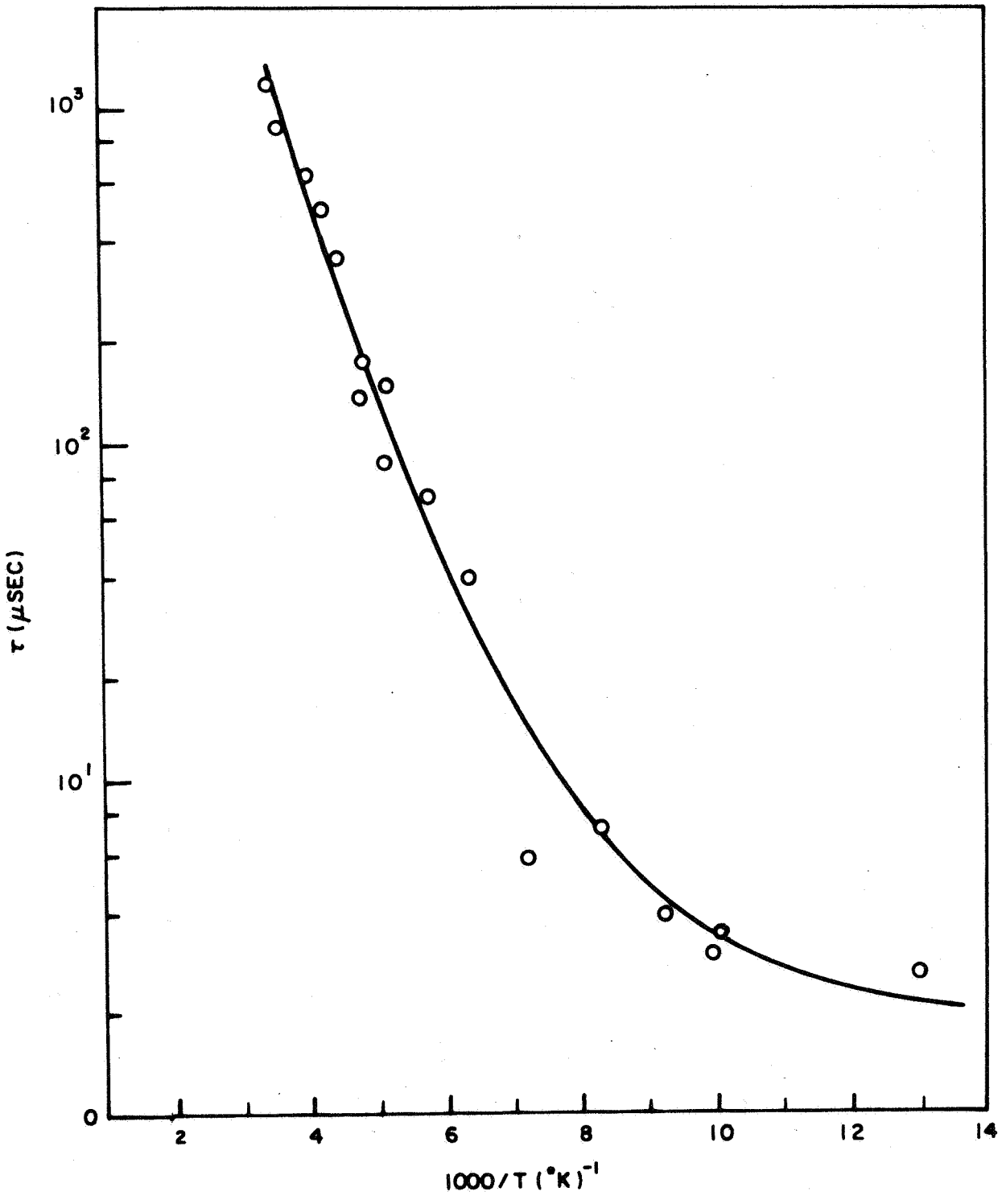

Fig. 17--Preirradiation temperature dependence of excess-carrier lifetime for p-type silicon

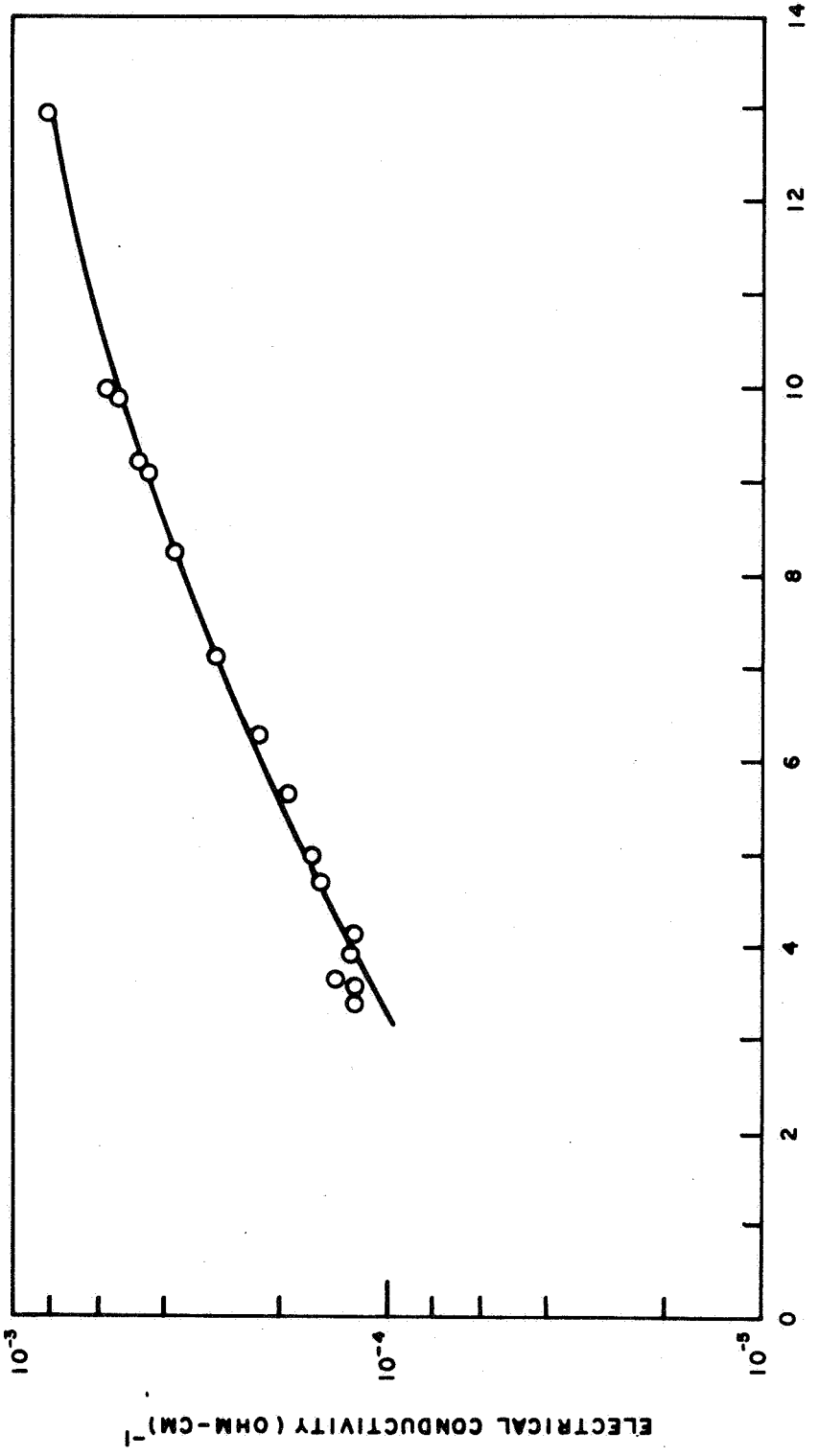

Fig. 18--Preirradiation temperature dependence of electrical conductivity for p-type silicon

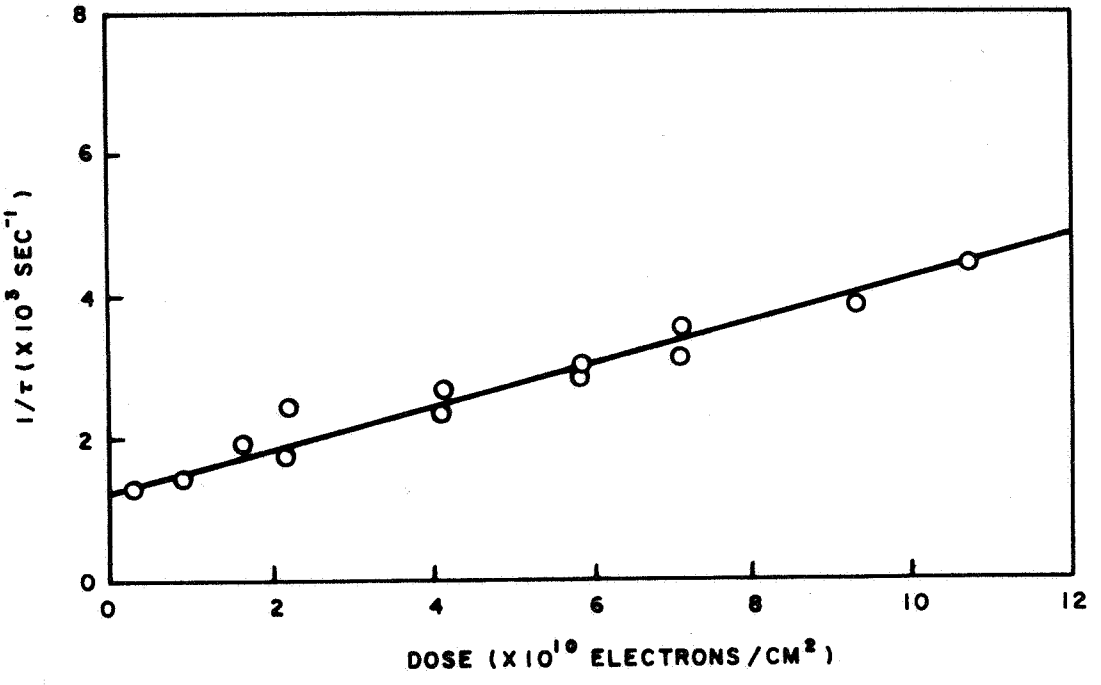

Fig. 19--Degradation of excess-carrier lifetime for p-type silicon after 30-MeV electron irradiation

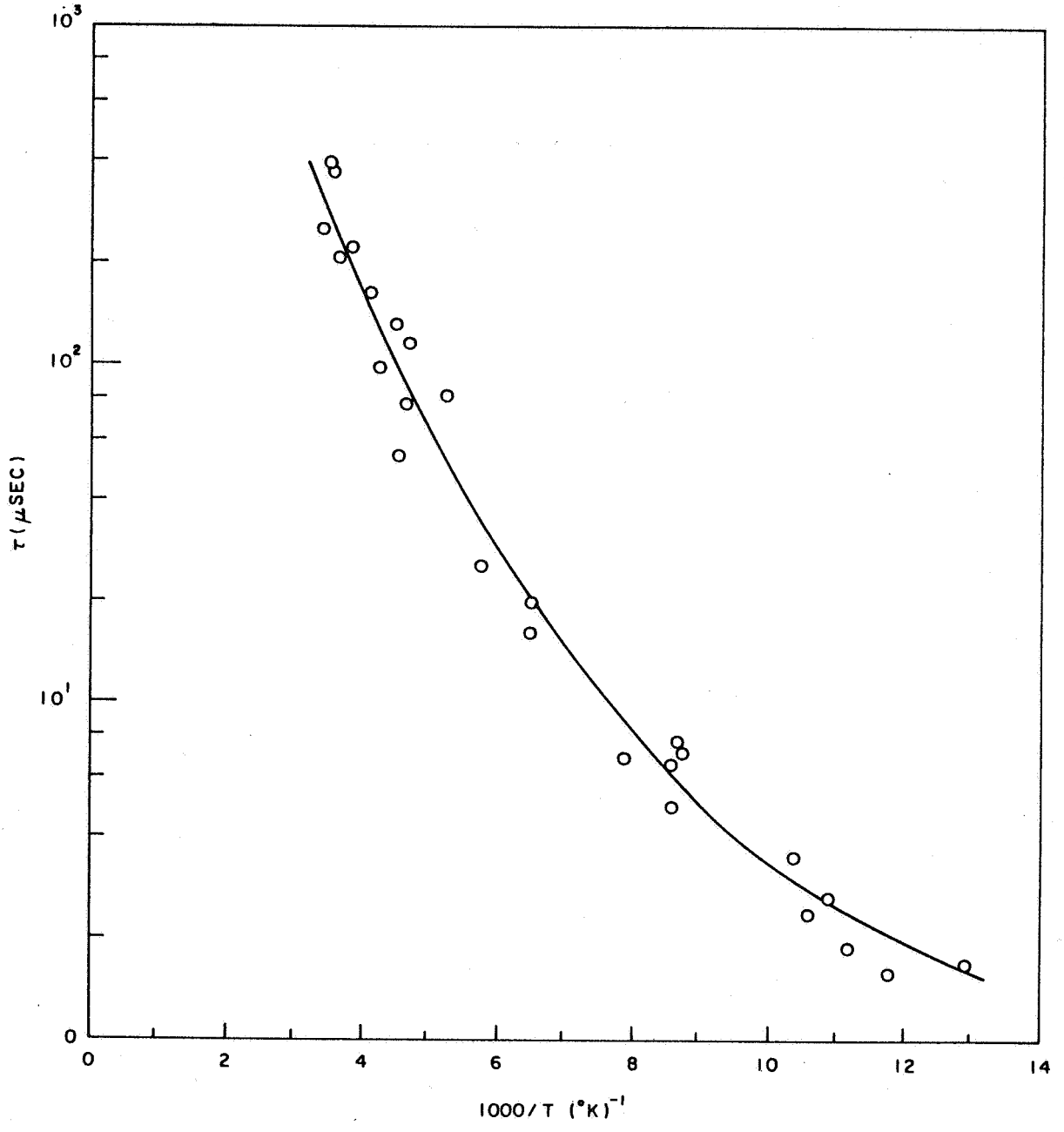

Fig. 20--Inverse temperature dependence of lifetime on p-type silicon after 30-MeV electron irradiation

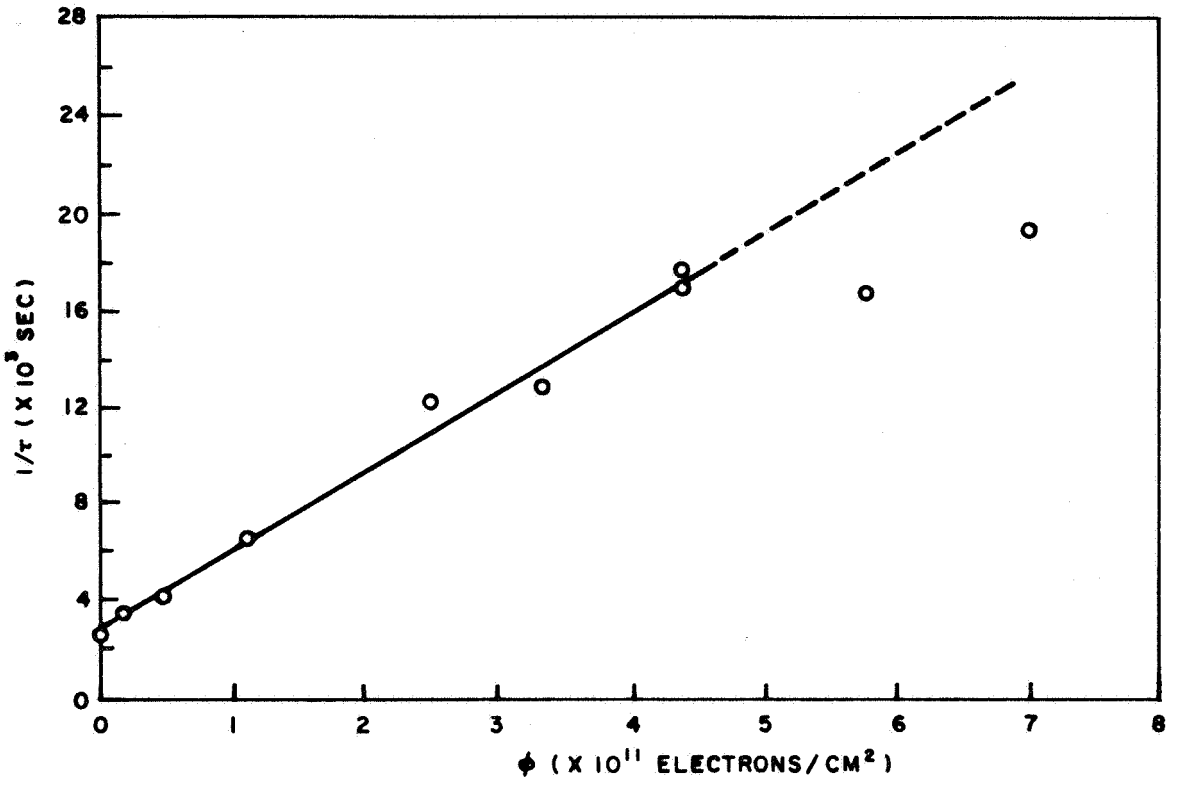

Fig. 21--Lifetime degradation for p-type silicon for 30-MeV electron irradiation

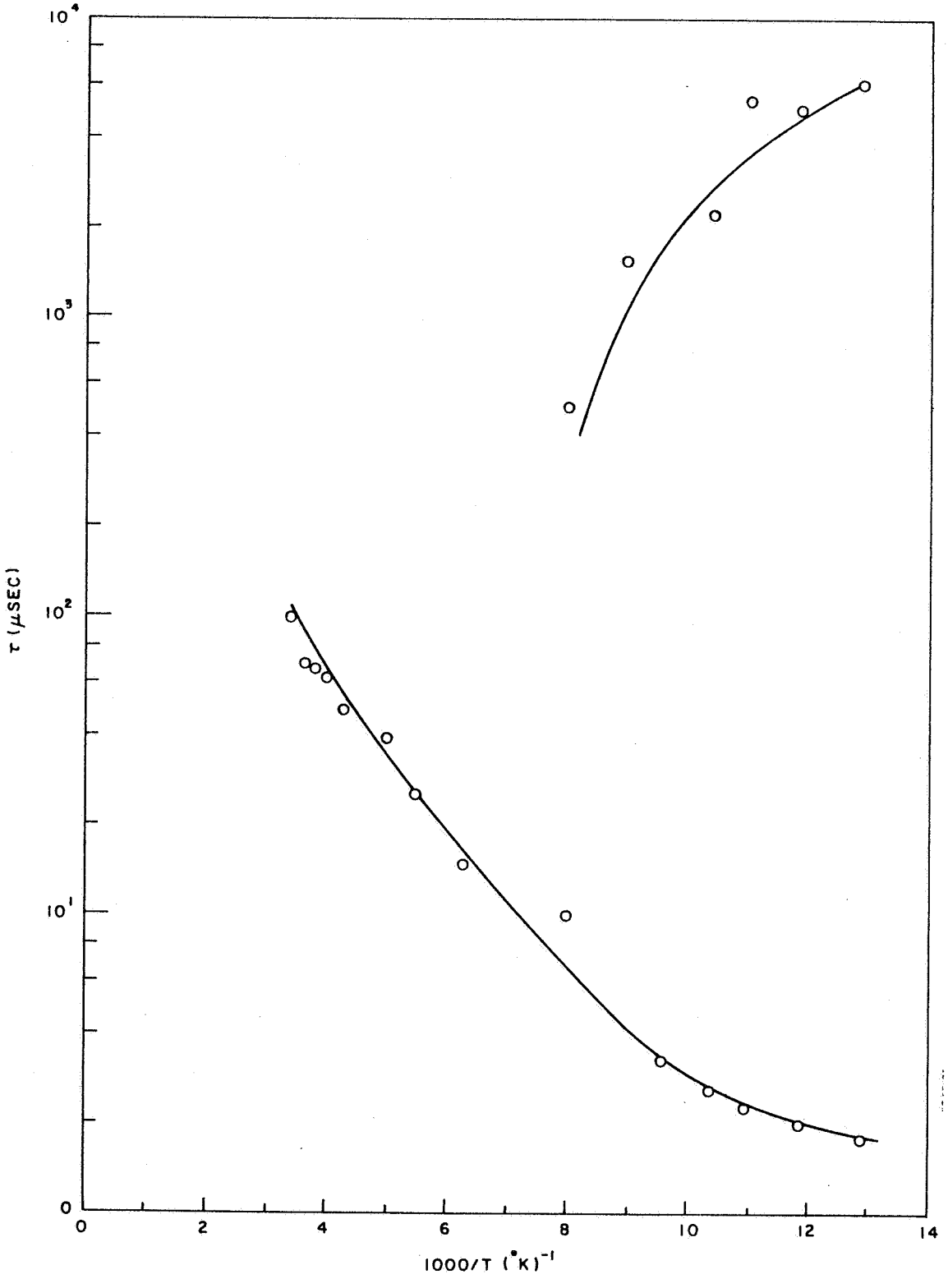

Fig. 22--Inverse temperature dependence of lifetime of p-type silicon after 30-MeV electron irradiation

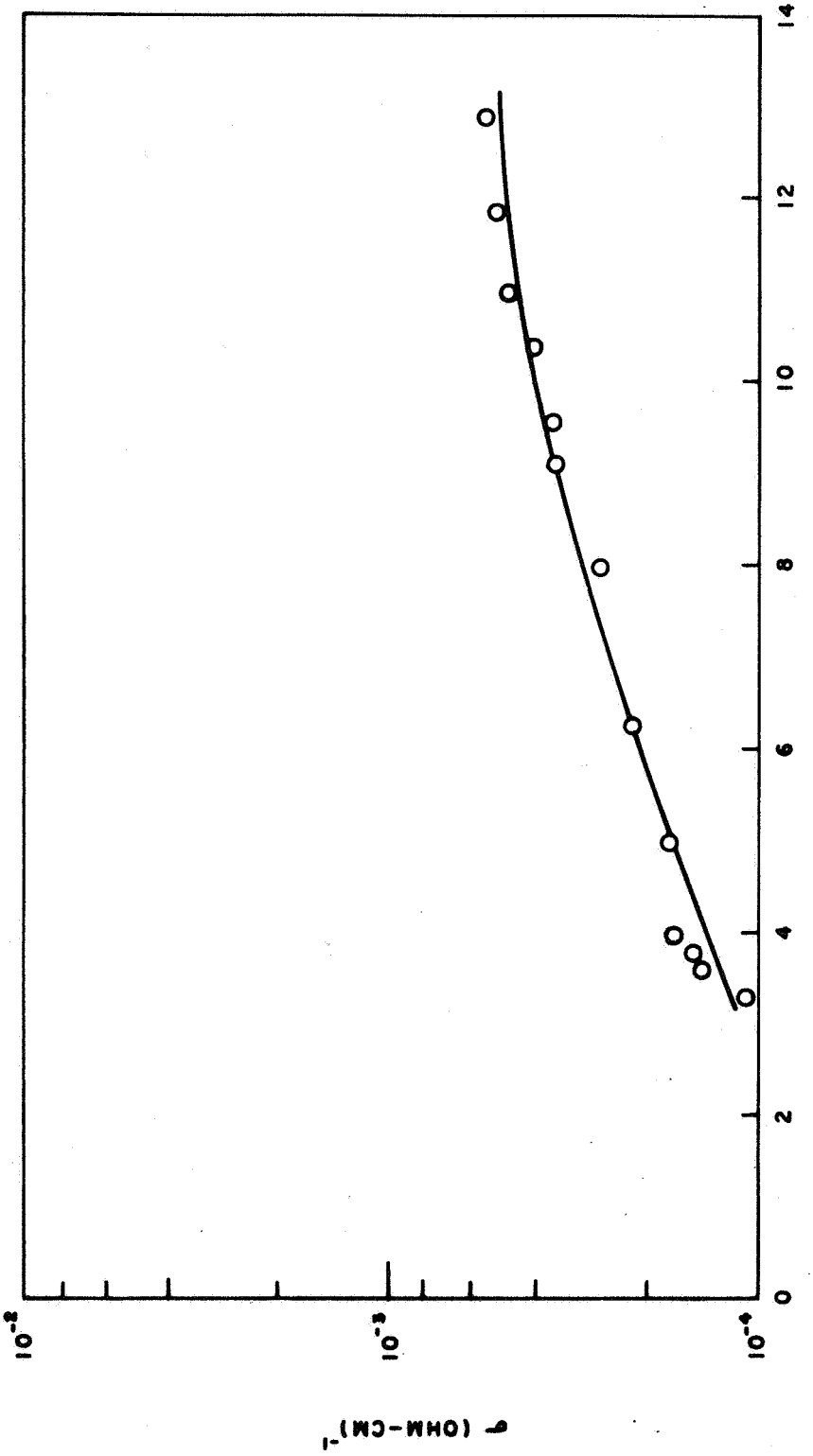

Fig. 23--Inverse temperature dependence of electrical conductivity after 30-MeV irradiation for p-type silicon

p-type silicon by 30-MeV electron irradiations are of primary concern in this investigation. These properties are discussed here.

3.4.1. n-type Silicon

To investigate the characteristics of the radiation-induced center, the lifetime of the carriers recombining through this center, τ_D, can be obtained from the measurement of the lifetime before irradiation, τ_0, and the lifetime, τ, after the fluence, Φ. With

$$\frac{1}{\tau} = \frac{1}{\tau_0} + K\Phi = \frac{1}{\tau_0} + \frac{1}{\tau_D} ,$$

$$\tau_D = \frac{\tau_0 - \tau}{\tau_0 \tau} .$$

Using the data for the low-injection-level lifetime from Fig. 4 for τ_0 and the data from Fig. 12 for values of τ, it is possible to determine the temperature dependence of τ_D after a fluence of 4.76×10^{11} electrons/cm^2, as shown in Fig. 24.

The Shockley-Read recombination theory (discussed in Section II) for the low-injection-level lifetime can be simplified for this high-resistivity n-type material and the temperature range from liquid nitrogen to 300°K. If the defect is in the upper half of the energy gap, then $p_1/n_0 \ll 1$; if the defect is in the lower half of the gap, then $n_1/n_0 \ll 1$. In the range from liquid-nitrogen to room temperature, the carrier concentration is about 2×10^{11} cm^{-3}. The temperature dependence of τ_D (see Fig. 24) exhibits no exponential temperature dependence, and thus both $n_1/n_0 \ll 1$ and $p_1/n_0 \ll 1$, depending on whether the recombination level is in the upper or lower half of the gap. Therefore, the low-injection-level lifetime temperature dependence can be analyzed using $\tau_{p_0} = 1/N_R v_{th} \sigma_p$.

For this ultrapure material, it should be kept in mind that in temperature cycling the sample from liquid-nitrogen to room temperature, the

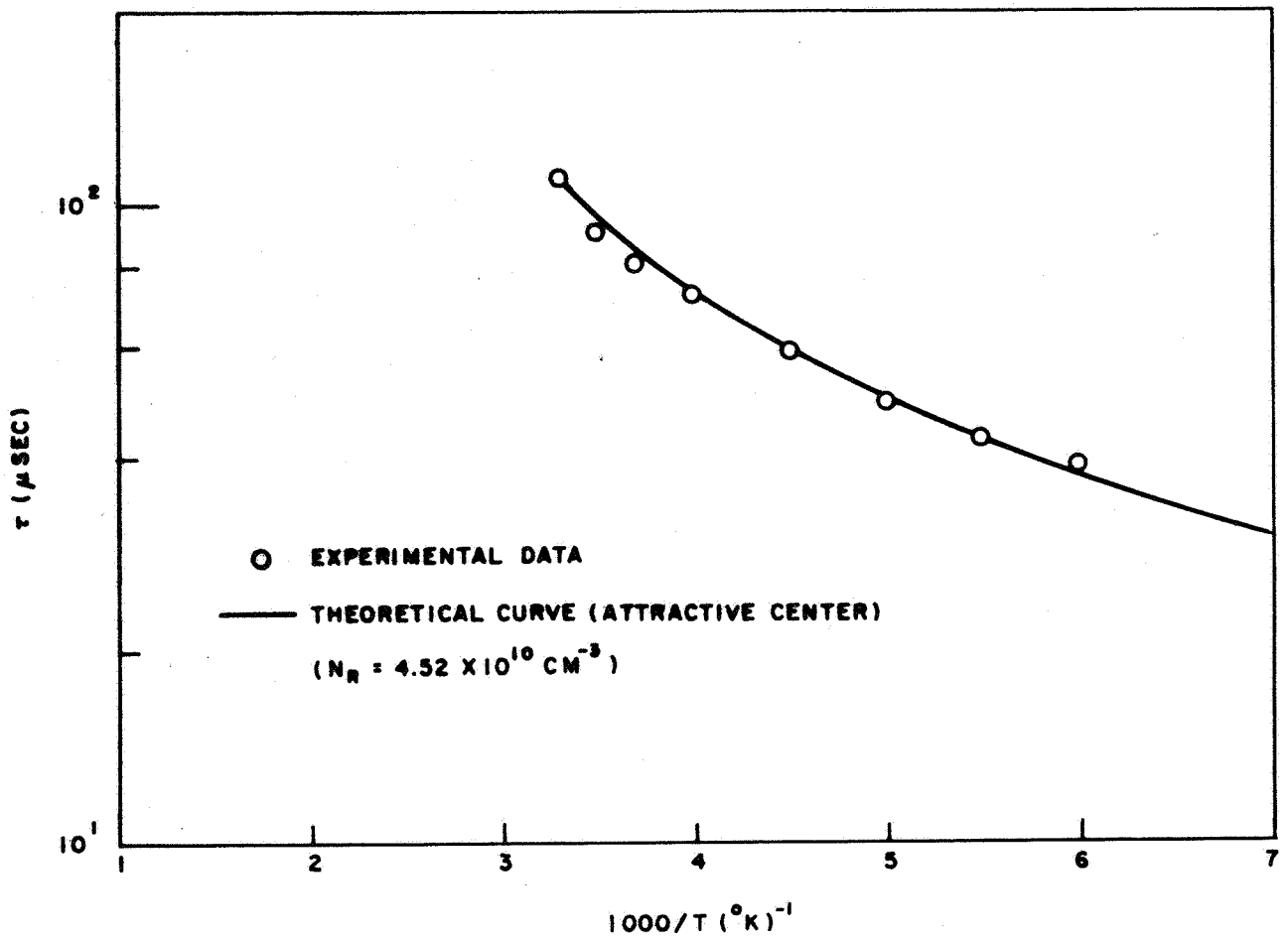

Fig. 24--Inverse temperature dependence of carrier lifetime for recombination through radiation-induced defect in n-type silicon

Fermi level moves from 0.15 eV to 0.48 eV below the conduction band.

Using the temperature dependence of the capture cross section of Lax for a singly attractive center and a carrier thermal velocity temperature dependence of $T^{1/2}$, it is possible to fit the experimental data with a theoretical curve. The theoretical curve shown in Fig. 24 represents a defect concentration of 4.52×10^{10} cm^{-3} after a fluence of 4.76×10^{11} electrons/cm^2. The capture cross section for this attractive center is about 1.3×10^{-14} cm^2 at room temperature. Since there is no exponential temperature dependence of the lifetime over the temperature range in which the Fermi level sweeps from 0.15 eV to 0.48 eV below the conduction band, the defect level lies at a depth greater than 0.50 eV from either band edge or within 0.05 eV of the center of the gap. Work by various other investigators using other techniques have also found deep levels in irradiated silicon.[19, 20, 1] The introduction rate of this deep-lying recombination center can be calculated from the measured fluence and from the number of recombination centers calculated by the Shockley-Read theory and the Lax cross section. This defect introduction rate is

$$\frac{\Delta N}{\Delta \Phi} = 0.095 \pm 0.02 \text{ cm}^{-1} .$$

The carrier removal rate obtained from electrical conductivity measurements when mobility changes are assumed small is

$$\frac{\Delta n}{\Delta \Phi} = \frac{1}{e\mu} \frac{\Delta \sigma}{\Delta \phi} = 0.18 \pm 0.05 \text{ cm}^{-1} .$$

The values of the carrier removal rate and defect introduction rate indicate that the deep-lying defect responsible for lifetime degradation may be associated with carrier removal. The fit of the experimental lifetime data with the capture cross section for an attractive center indicates that the recombination center is attractive to holes. Thus, the deep-lying defect produced in high-purity n-type silicon may be produced as an acceptor; this acceptor removes carriers from the conduction band, which becomes negatively charged. This is then the attractive center through which the minority carriers

recombine. The isochronal annealing of the degraded lifetime shows a gradual recovery commencing about 360°K. The broad temperature range over which this annealing occurs indicates that the annealing is not a simple process with a single activation energy, but that it involves a spectrum of energies.

The trapping center appearing at low temperatures does not affect the recombination properties at room temperature. Extensive research will have to be performed on this trapping center before more can be determined about its properties.

3.4.2. p-type Silicon

The nature of the recombination center introduced in p-type silicon by 30-MeV electrons at room temperature is determined in the same manner as that for n-type silicon. The low-injection-level lifetime due to the irradiation-introduced center (τ_D) is plotted in Fig. 25. An attempt has been made to fit the experimental data using the Shockley-Read recombination theory (see Section II) along with the singly attractive cross section of Lax. Depending on whether the center is in the upper or lower half of the gap, $p_1/p_0 \ll 1$ or $n_1/p_0 \ll 1$ for the carrier concentration of 1×10^{12} cm^{-3}. Since there is no detectable exponential temperature dependence of the lifetime data, $n_1/p_0 \ll 1$ and $p_1/p_0 \ll 1$ and the temperature dependence of the lifetime is $\tau_{n_0} = 1/N_R v_{th} \sigma_n$. This theoretical temperature dependence of lifetime is plotted in Fig. 25. The theoretical curve represents a defect density of 5.9×10^{10} cm^{-3} for a fluence of 8.05×10^{11} electrons/cm^2 and an assumed attractive cross section of 10^{-14} cm^2 at room temperature. This cross section is obtained from the theory of Lax.

In this high-resistivity p-type silicon, the Fermi level sweeps from 0.1 eV to 0.41 eV above the valence band during temperature cycling from 77.5°K to room temperature. The nonappearance of an exponential temperature dependence on the lifetime indicates that this recombination center

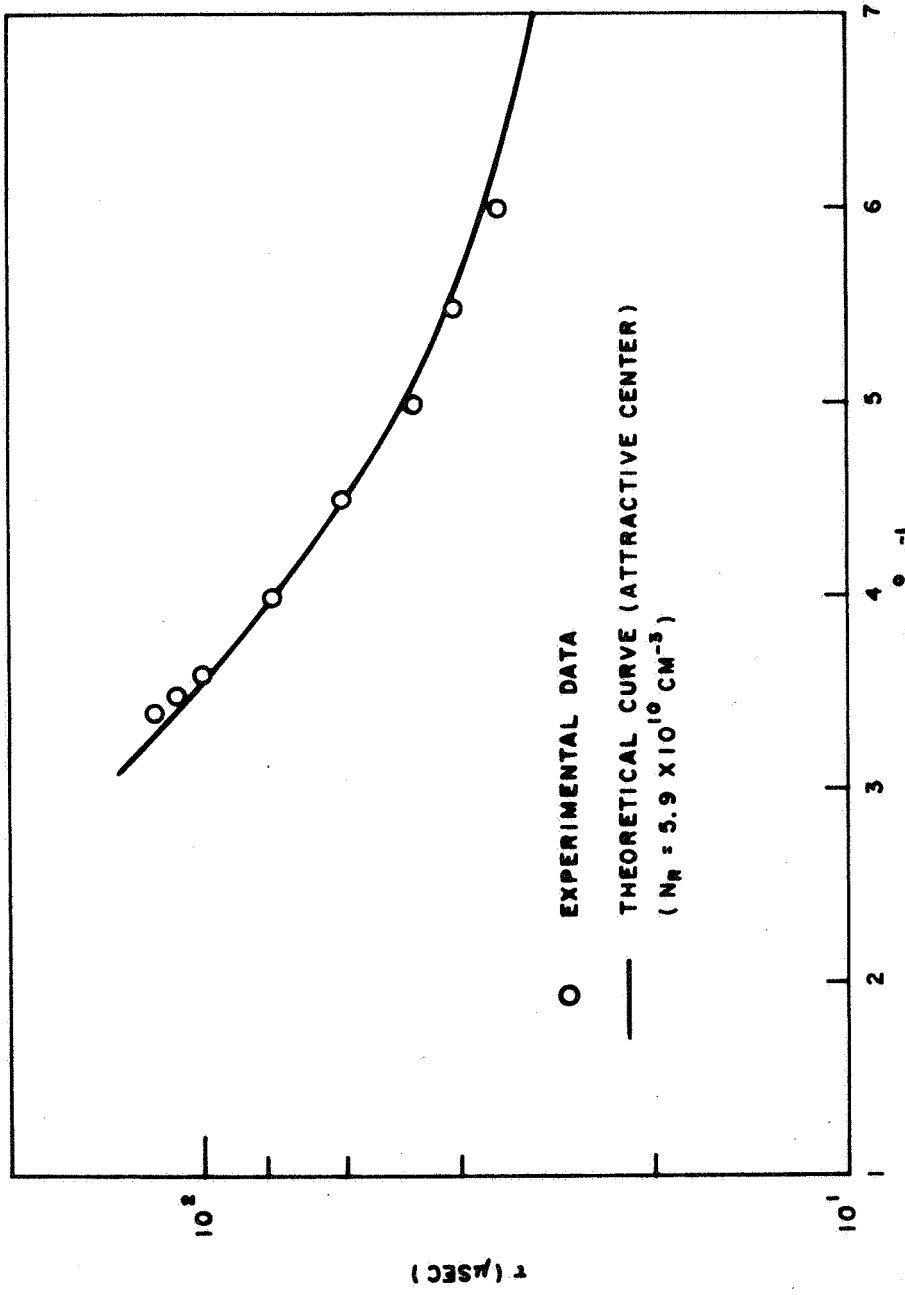

Fig. 25--Inverse temperature dependence of carrier lifetime for recombination through radiation-induced defect in p-type silicon

is greater than 0.45 eV from either band edge, i.e., within 0.10 eV of the center of the gap.

The recombination-center introduction rate is

$$\frac{\Delta N}{\Delta \Phi} = 0.073 \pm 0.02 \text{ cm}^{-1} .$$

The carrier removal rate for this material as measured from changes in electrical conductivity is

$$\frac{\Delta p}{\Delta \Phi} = 0.25 \pm 0.05 \text{ cm}^{-1} .$$

The values of the defect introduction rate and carrier removal rate suggest that the defect responsible for the lifetime degradation may be associated with majority carrier removal.

For the p-type material, the deep-lying defect recombination center introduced by the electron irradiation would be a donor state that would remove holes from the valence band. This carrier removal would charge the center positively, making it an attractive center for the capture of electrons. This center would be the center responsible for degradation of carrier lifetime in our p-type material.

3.5. CONCLUSIONS

The 30-MeV electron irradiations of ultrapure n- and p-type silicon were performed in an attempt to determine the nature of the intrinsic defects that are active as recombination centers. It was hoped that the high purity of the material would eliminate the production of the multitude of defects[22] that are impurity-dependent, and that the deep-lying Fermi level in high-resistivity material would reveal the energy level of the defect.

The use of the microwave-reflection technique to measure the quiescent and transient electrical conductivity was an initial attempt to eliminate the "contact problem" in radiation-effects studies on silicon.

These experiments have shown that the microwave absorption technique is very useful in the measurement of the temperature-dependent electrical properties of silicon as long as certain limitations are obeyed. Further extension of this technique will no doubt make it very useful for measurements on dielectrics.

In both the n- and p-type silicon, it was found that the lifetime data on irradiated samples could be analyzed by the Shockley-Read recombination theory using the capture cross sections of Lax. In both materials, the recombination center was very near the center of the gap--in the n-type material, within 0.05 eV of the center, and in the p-type material, within 0.10 eV of the center. The p-type material had a slightly larger lifetime degradation constant. The deep-lying recombination center was attractive to minority carriers in both cases.

It is known that silicon appears to approach intrinsic behavior on prolonged exposure. This suggests that the dominant defects--acceptors and donors--are located on either side of the center of the forbidden energy gap.

The defect introduced by the 30-MeV irradiation in these experiments may be this intrinsic defect. The defect is introduced in both materials as a majority-carrier acceptor; once the defect has removed a majority carrier from the respective band, the center is then an attractive recombination center for the minority carriers. Whether the defects in the n- and p-type materials are two states of the same defect or two different defects has not been determined at the present time.

IV. DC CONDUCTIVITY MEASUREMENTS

4.1. ELECTRICAL CONTACTS

One of the problems encountered in the dc conductivity technique for measuring carrier lifetimes on low-resistivity n- and p-type silicon has been with the contacts to the silicon samples, especially at 80°K where the contact resistance increases. The effects of bad contacts show up in several ways. One is the photovoltages induced by the ionizing radiation and observed when there is no current through the sample. Such a voltage must be small in comparison to any expected change in voltage with current through the sample in order to be neglected. If such a voltage is not small, then it must be subtracted from the observed signal. Another effect occurs when the contact resistance to the sample changes much more than the sample resistance. A third effect results when contact resistance, together with circuit capacitance, causes relaxation times which mask short lifetimes. Both of these effects have been discussed in the previous summary report.[2]

In previous experiments, the voltage probes to n-type samples were made by alloying As-doped gold wires or preforms at 450°C, and this method is still being used. The current leads, which were previously electroplated nickel, are also gold-alloyed now. The plated nickel contacts, although lower in resistance than the gold-alloy contacts at room temperature, have a higher resistance at 80°K. The lower resistance at room temperature may be explained by differences in spreading resistances, as the electroplated contacts have larger areas than do the alloy ones. It was observed that the resistance of the electroplated contacts increases with decreasing temperature, but the resistance of the gold-alloyed contacts decreases by about a factor of ten or so. Since the resistivity of the

sample also decreases by about a factor of ten, the effect of the contact might be comparable at 300°K and 80°K. The measurements on n-type samples indicate that the contact problem is not a major one now.

Contacts on p-type silicon, however, is still a problem. Presently, B-doped gold-alloy wire is being used for contacts. Although the resistance of these contacts also decreases by a factor of ten from room temperature to 80°K, a large photovoltage appears at the lower temperature. Apparently, a decrease in contact resistance is not a good test for photovoltages. Current-voltage (I-V) curves were taken of these contacts using a transistor curve tracer. The two current contacts and one voltage probe were used as terminals, as shown below, for the measurement of contact resistance.

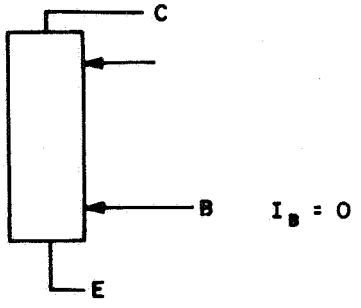

A curve of I_C versus V_B with base current $I_B = 0$ gives the sum of the contact resistance at E and the sample resistance to B. The sample resistance and spreading resistance should be ohmic, and any nonlinearity in the I-V curves should be due to the semiconductor-metal contact.

The B-doped gold-alloy contacts showed a slightly nonlinear trace at room temperature; they showed slightly more nonlinearity at 80°K. Samples using this contact had photovoltages that were small at room temperature but much larger at 80°K.

Aluminum was also tried as a contact. Evaporation of Al plus alloying at 600°C, Al ion implantation plus alloying at 600°C, and Al preforms alloyed at 600°C were used on various samples. Only the I-V curve of the ion-implantation sample was nonlinear; this occurred at room temperature, but it was linear at 80°K, which at present seems odd. These contacts show promise, but lifetime experiments on these samples have not yet been made.

The p-type sample used in the lifetime experiments had B-doped gold-alloy contacts. For the reasons given above, the measurements were limited to the higher temperatures.

4.2. EXPERIMENTAL TECHNIQUES

The sample chamber used in the dc conductivity experiments was described in a previous report.[23] A discussion of sample preparation also was included in that report as well as in subsequent reports.[24, 2] The sample is a standard bar configuration with two current contacts and two voltage probes with a thermocouple attached either to a current contact or to a voltage contact.

Two different circuits were used on the samples reported herein. Initially, the circuit described in Ref. 2 was used. However, as the low-injection-level capabilities of that circuit were not necessary for the present experiments, a simpler circuit was used. Essentially, the current pulser and its related trigger circuits were replaced by a dc voltage source. This is shown in Fig. 26. As before, whenever lifetime decays were taken, the long dc measuring lines were disconnected to minimize any noise pickup. A cathode follower was close to the sample so that the capacitance of the measuring leads were also minimized.

4.3. EXPERIMENTAL RESULTS

4.3.1. n-type Silicon

In the last summary report,[2] it was concluded that the dominant

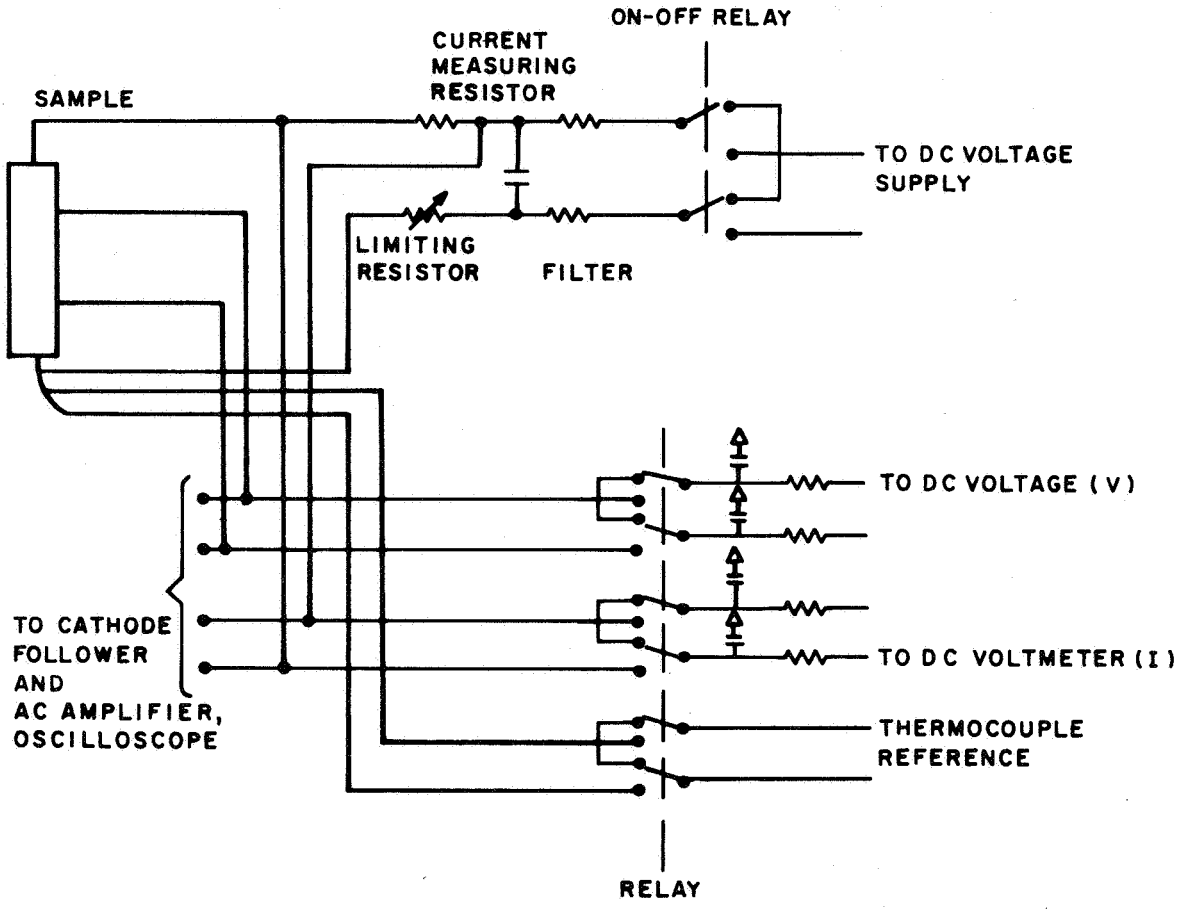

Fig. 26--Lifetime measuring circuit

recombination center in 10-ohm-cm P-doped silicon irradiated by 30-MeV electrons is neither the substitutional oxygen nor the vacancy-phosphorus complex. The divacancy was also ruled out because of introduction-rate considerations. It was then concluded that the center was a net acceptor with an ionization energy greater than 0.40 eV which had an introduction rate greater than 0.19 cm^{-1}. It was also concluded that there was no significant difference between quartz-crucible (QC) grown silicon and floating-zone (FZ) refined silicon in the introduction rate or in the temperature dependence of the low-injection lifetime.

In order to verify and extend these results, samples of higher resistivities were used. It was then possible to sweep the Fermi level through a wider range and possibly cross the recombination center. Measurements of intensity dependences at various temperatures would also make it possible to obtain information about the electron and hole capture cross sections. Two P-doped, 50-ohm-cm silicon samples, one of which was QC grown and the other FZ refined, were used for the experiments.

The QC-grown sample was irradiated with 30-MeV electrons at 300°K. The damage curve is shown in Fig. 27. A value of $(\Delta 1/\tau)/\Delta\phi = 4.8 \pm 0.5 \times 10^{-8}$ cm^2/electron sec was obtained. The low-level lifetime versus temperature was taken before and after the irradiation. In all cases, the sample was taken to about 100°C for 5 min immediately after irradiation and before any lifetime versus temperature measurements were made. The lifetime versus temperature curves are shown in Fig. 28. The dependence of the carrier lifetime as a function of excess carrier concentration at four different temperatures is shown in Fig. 29.

It should be noted in Fig. 28 that the preirradiation curve and postirradiation curves differ by a factor of about eight at room temperature but converge at lower and higher temperatures. This implies that the

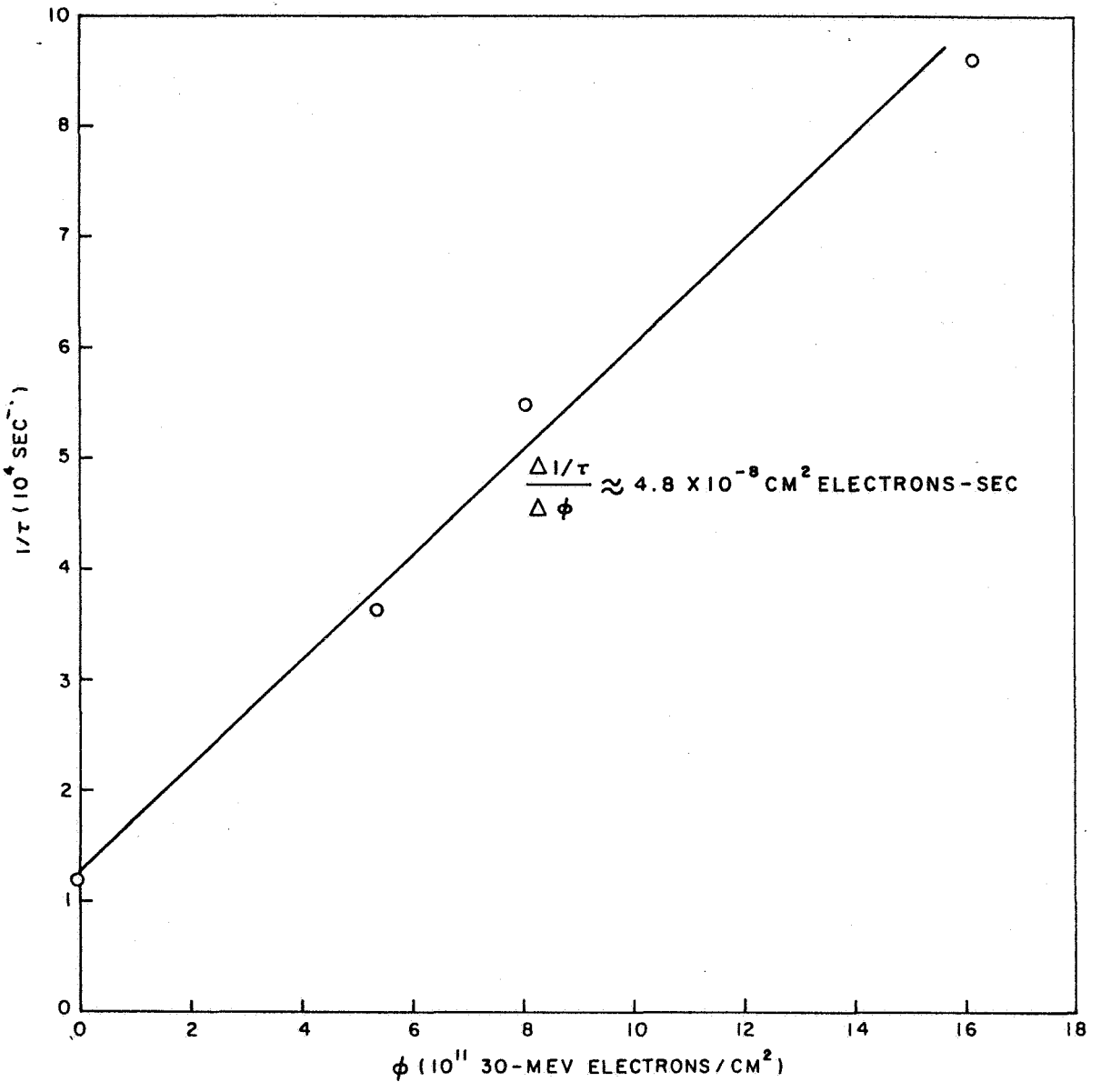

Fig. 27--Inverse lifetime vs integrated electron flux at 300°K for 50-ohm-cm, P-doped, QC silicon

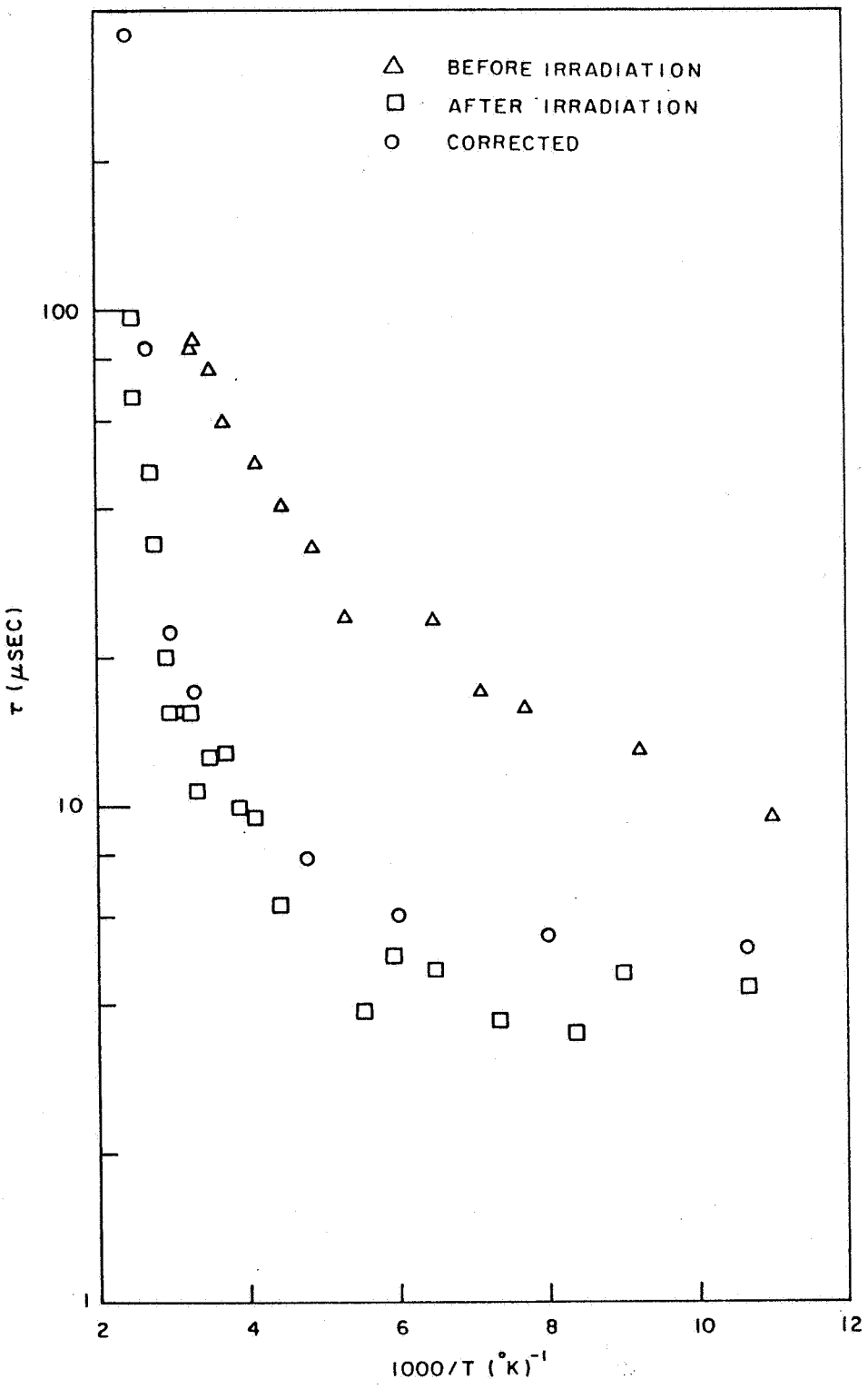

Fig. 28--Low-level lifetime vs reciprocal temperature for 50-ohm-cm, P-doped, QC silicon

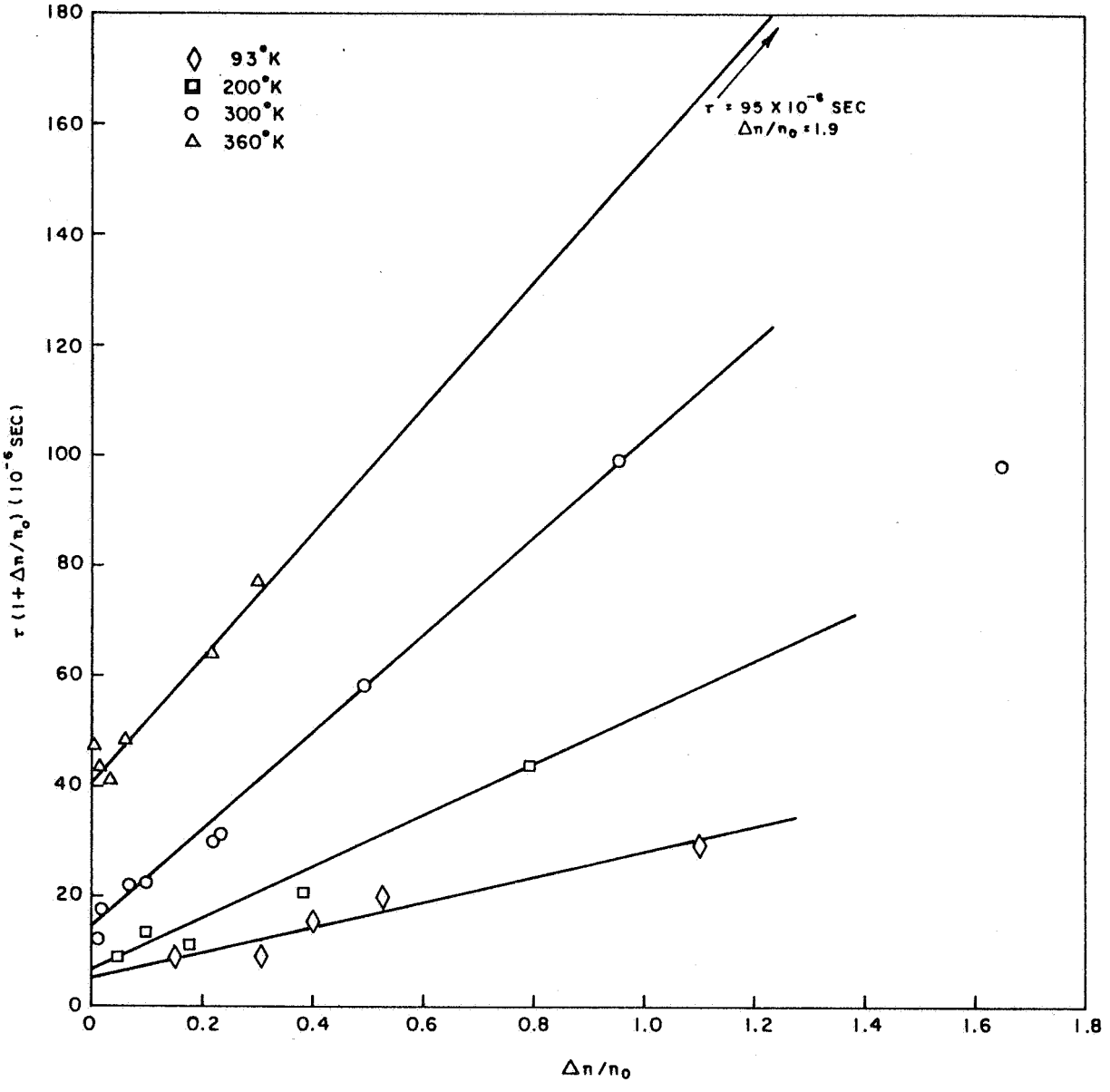

Fig. 29--Dependence of lifetime on excess carrier concentration for 50-ohm-cm, P-doped, QC silicon

measured lifetimes at these temperatures have an appreciable component due to the recombination centers in the unirradiated material. Therefore, assuming

$$\tau_D = \left(\frac{1}{\tau} - \frac{1}{\tau_0}\right)^{-1},$$

where τ is the measured lifetime, τ_0 is the lifetime in the unirradiated sample, and τ_D is the lifetime due to the irradiation-introduced defects, the experimental data is corrected and τ_D (corrected lifetime) is shown in Fig. 28. The curves of Fig. 29 were also corrected in this way. Such a correction in this case is not entirely correct, but it seems to be satisfactory for the present. The data obtained from Fig. 29 is summarized in Table 1.

Table 1

Temperature (°K)	τ_ℓ (μsec)	τ_h (μsec)	τ_h/τ_ℓ
93	5.4	22	4.1
200	6.5	47.5	7.3
300	15	92	6.1
360	43	120	2.8

Another piece of information needed to fit the Shockley-Read theory would be the depth of the recombination center in the forbidden gap. Such a level can be obtained from the slope of the exponential in Fig. 28. However, since the postirradiation lifetimes were comparable to the preirradiation lifetimes, such a determination of the level would have a large error. Therefore, the recombination level will not be used as a known parameter.

In the present analysis, it was assumed that the simple one-level Shockley-Read theory applies. The fact that the injection dependence curves of Fig. 29 are linear supports this assumption. Therefore, the

τ_ℓ should follow either $\tau_{p_0}(1 + n_1/n_0)$ or $\tau_{p_0} + \tau_{n_0}(p_1/n_0)$.

The case in which the recombination level is above the center of the gap is considered first. In this case, $\tau_\ell = \tau_{p_0}(1 + n_1/n_0)$ and $\tau_h = \tau_{p_0} + \tau_{n_0}$. Using the theoretical temperature dependence of an attractive center as derived by Lax[4] and using three energy values for the position of the recombination level in the energy gap, we obtain Fig. 30. The data at the lowest temperature in Fig. 28 was omitted since it was obvious that the lower points could not be fitted. Figure 30 shows the level to be 0.38 ±0.01 eV. Similar calculations in which a neutral center was assumed did not fit the data.

Using the value of $E_R = 0.38$ eV and the values for τ_h and τ_ℓ in Table 1 and solving for τ_{p_0} and τ_{n_0}, we get Fig. 31. The curves for the theoretical temperature dependence of the capture cross section times the velocity of the carrier are also plotted in Fig. 31. As can be seen, the point at 90°K does not fit the theoretical curve for the attractive center. This could be due to an increase in lifetime at lower temperatures (Fig. 28), which was also observed in 7-ohm-cm, QC silicon.[2] Disregarding the low-temperature point, these theoretical results indicate that the neutral cross section needed to fit the experimental data is steeper than that predicted by theory.

If we assume the energy level to be below the center of the gap, then $\tau_\ell = \tau_{p_0} + \tau_{n_0}(p_1/n_0)$ and $\tau_\ell = \tau_{p_0} + \tau_{n_0}$. At low temperature, such an assumption is consistent with the data, since in this region τ_{p_0} is the pertinent parameter independent of the position of the defect energy level. In order to fit a curve such as that in Fig. 30 for $\tau_\ell = \tau_{p_0} + \tau_{n_0}(p_1/n_0)$ versus reciprocal temperature, an estimate of τ_{n_0} and τ_{p_0} must be made. In the assumption that the level is in the upper half of the gap, the neutral center for τ_{p_0} was found not to fit the data. It is obvious that it will not fit the data for the level below the center of the gap either; so τ_{p_0} was

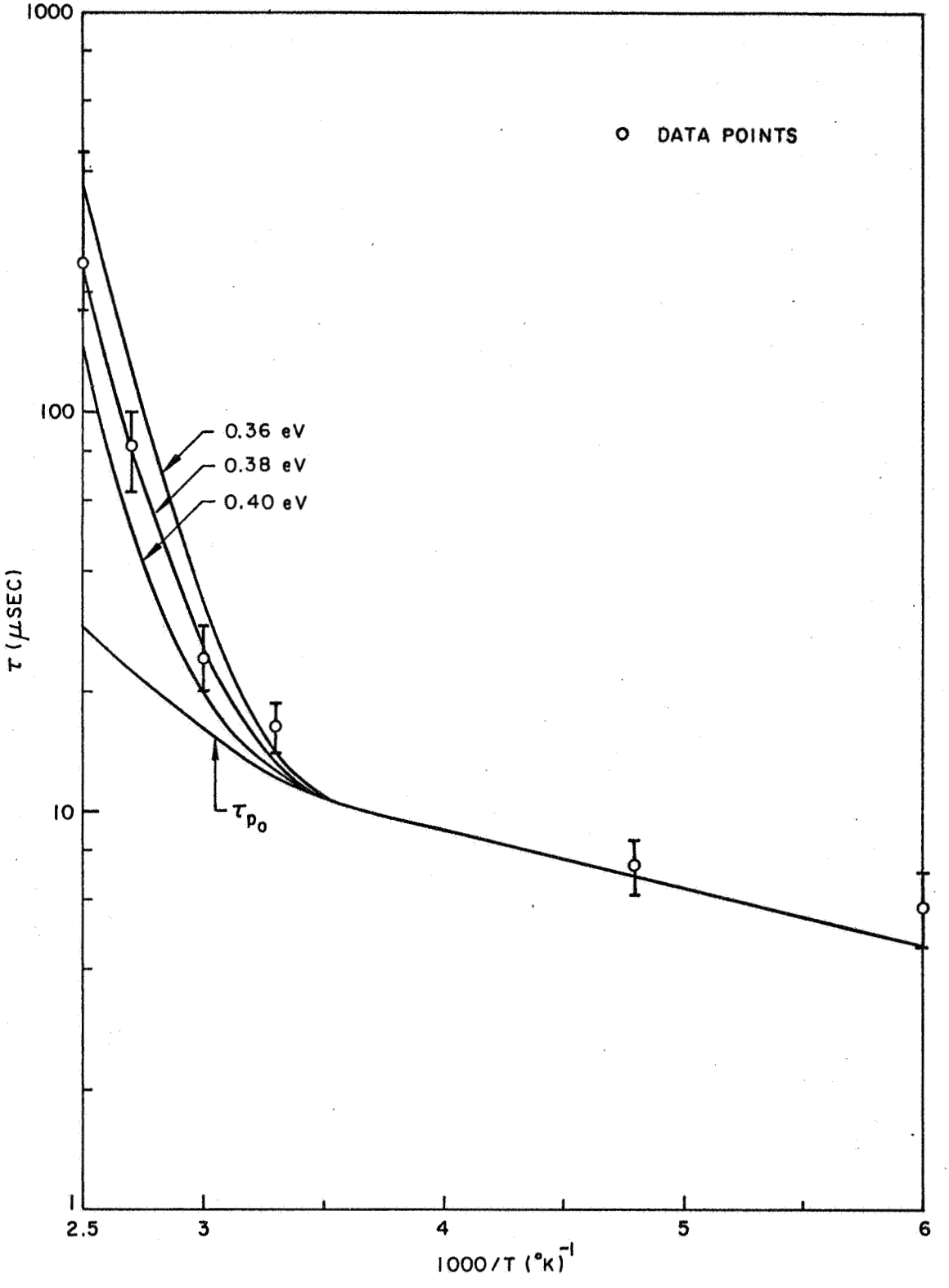

Fig. 30--Low-level lifetime vs reciprocal temperature for 50-ohm-cm, P-doped, QC silicon for recombination level above center of the gap

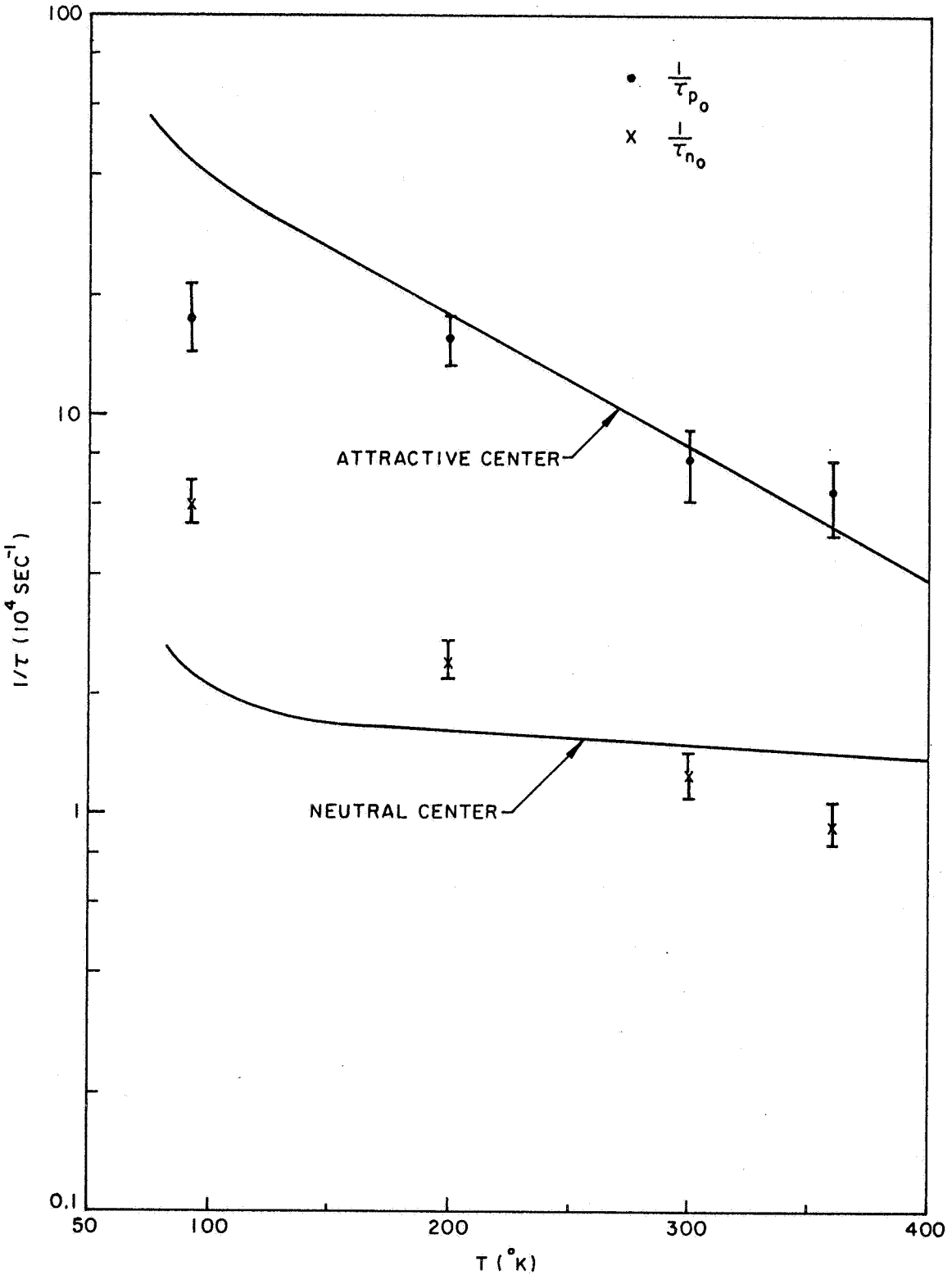

Fig. 31--Reciprocal lifetime vs temperature

assumed to be attractive, and the theoretical temperature dependence for an attractive center for τ_{p_0} was used. τ_{n_0} was estimated by using the theoretical temperature dependence for a neutral center and normalizing the ratio of $\tau_{p_0}/\tau_{n_0} = 6.3$ obtained from the injection dependence at 200°K. Various assumed values of E_R give Fig. 32, and from this figure, a value of 0.37 eV appears to be a good fit. However, if the injection-dependence result at 360°K is used, a negative value for τ_{p_0} is obtained. It is found that a level at least as deep as 0.41 eV is needed to obtain a result consistent with this injection dependence. The value 0.41 eV does not explain the data of Fig. 32. However, if a different temperature dependence for the neutral cross section is assumed, values of $E_R > 0.41$ eV can be fit to the data of Fig. 32, and this will be consistent with the injection dependence result at 360°K. Assuming so results in a temperature dependence that becomes increasingly steeper as one uses larger values of E_R. It can be seen that as E_R is increased, p_1/n_0 decreases such that more of the steep rise in τ at high temperatures in Fig. 32 must be explained by the temperature dependence of the neutral cross section.

A closer fit to theory for a recombination level above the center of the gap leads to the conclusion that the recombination level seen is an acceptor lying 0.38 ±0.01 eV below the conduction band.

A 50-ohm-cm- P-doped, FZ-refined silicon sample was also irradiated. Unfortunately, because of experimental difficulties, the sample lifetime was reduced considerably by the irradiation during setup and thus no plots of preirradiation lifetimes versus temperature or of lifetime versus flux were obtained. However, from previous experiments[2] it has been seen that the degradation rate of the lifetime is comparable to that in QC-grown material, but such a parameter is not particularly indicative of any difference in recombination properties.

The data for the FZ sample, after irradiation by an unknown amount, are shown in Figs. 33 and 34. It can be seen from Figs. 33 and 28 that the

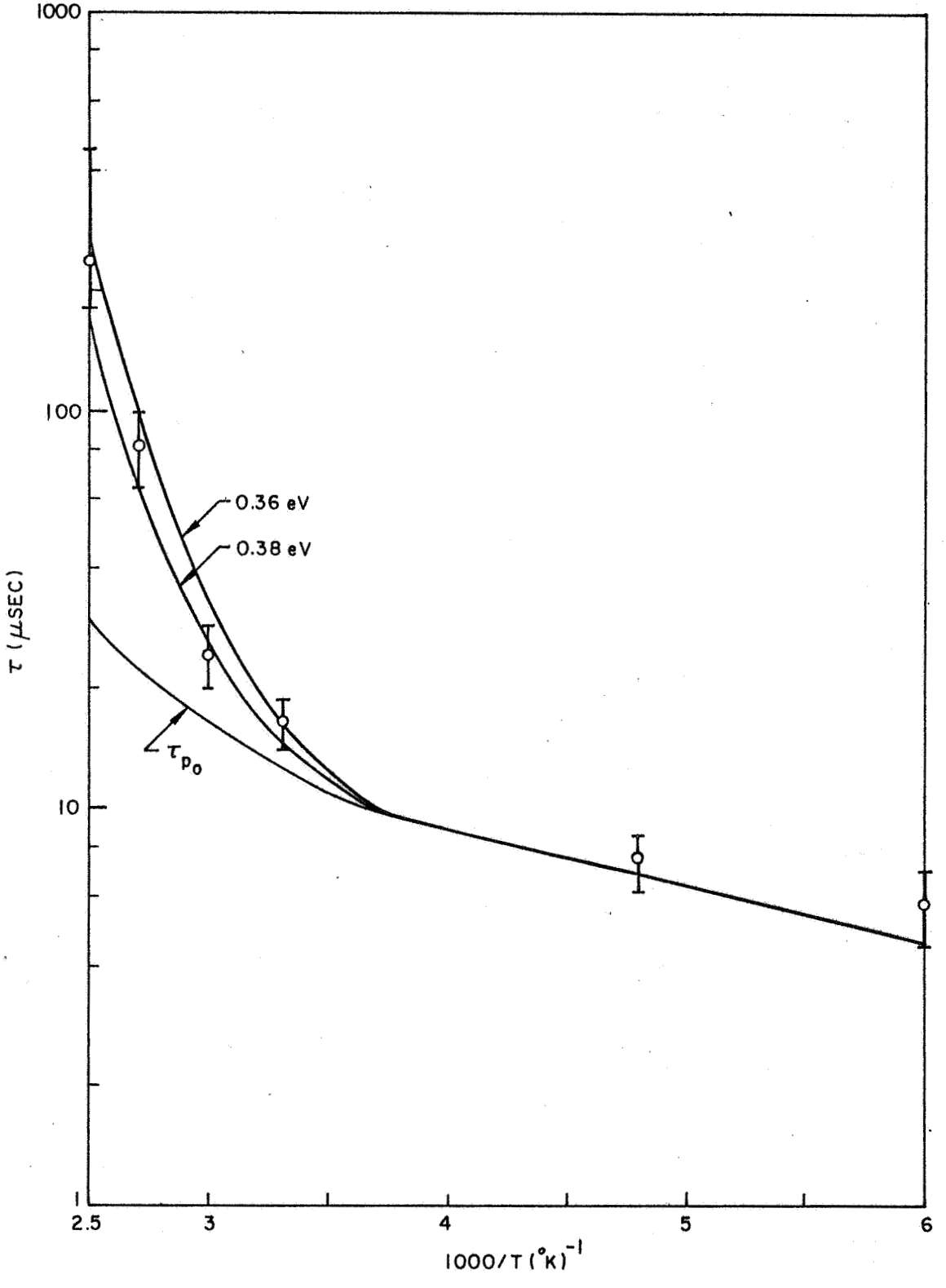

Fig. 32--Low-level lifetime vs reciprocal temperature for 50-ohm-cm, P-doped, QC silicon for recombination level below center of the gap

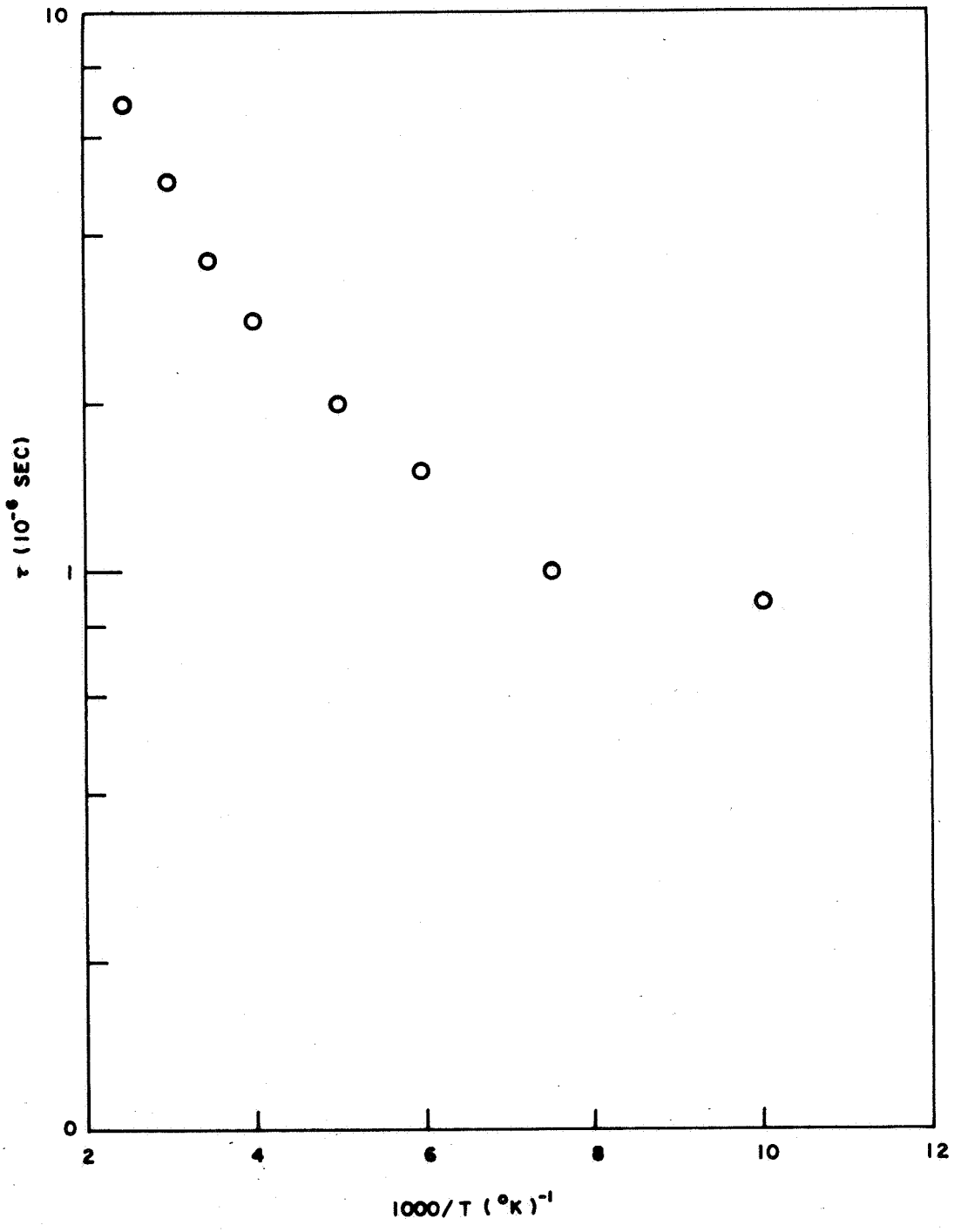

Fig. 33--Low-level lifetime vs reciprocal temperature for 50-ohm-cm, P-doped, FZ silicon

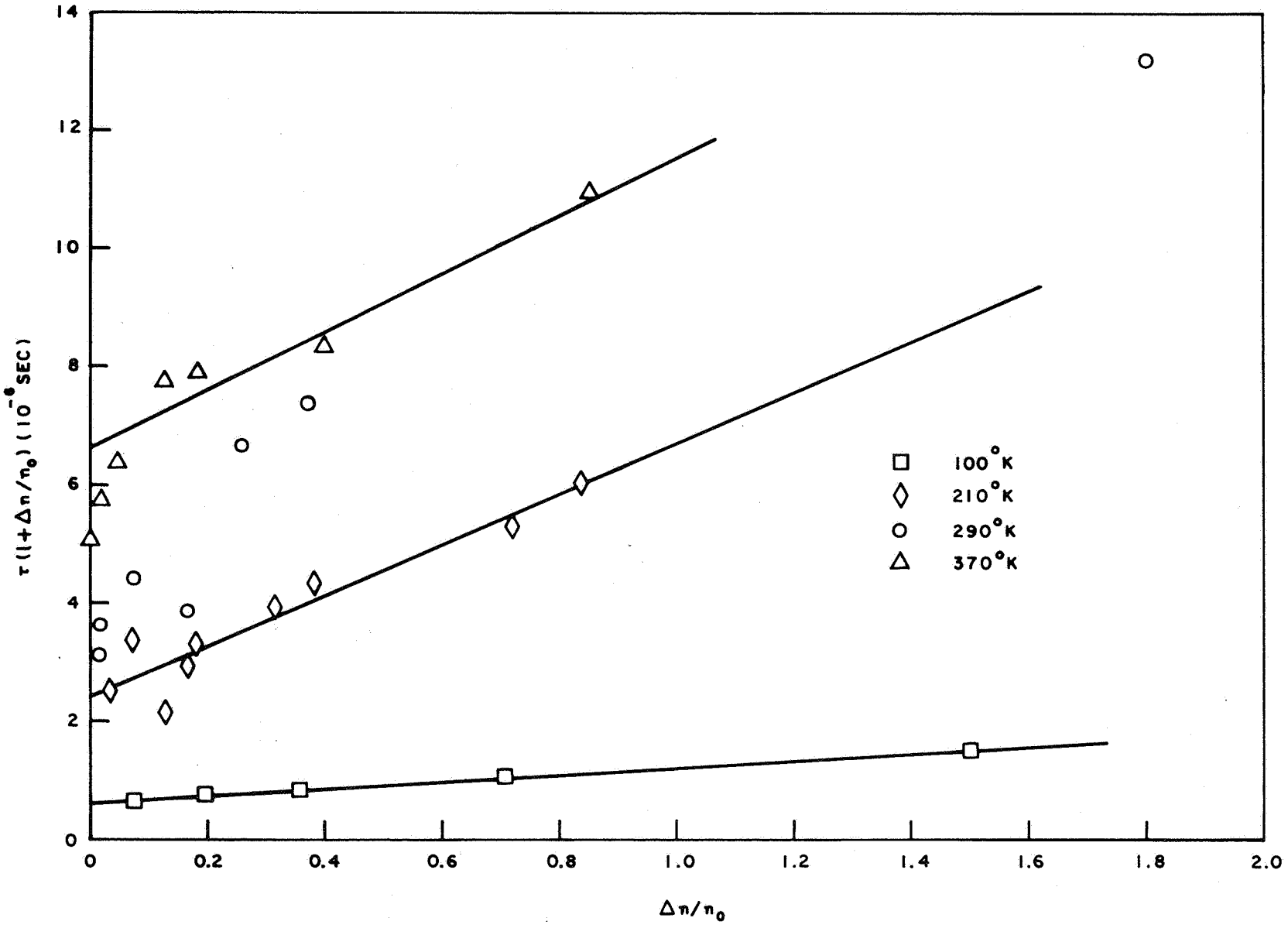

Fig. 34--Dependence of lifetime on excess carrier concentration for 50-ohm-cm, P-doped, FZ silicon

recombination center in the QC and FZ materials are different. The resistivities of the two samples were different by 30 percent, but this does not account for the differences in recombination observed.

Figure 34 also shows that the injection-dependence plots are linear at lower temperatures but that they become increasingly nonlinear with increasing temperature. This indicates that the simple, one-level Shockley-Read theory is not applicable at the high temperatures and probably not at the low temperatures. Therefore, a more complex model must be used.

The nonlinearity of the injection-dependence curves can be explained by (1) a two-level recombination center or (2) two recombination centers. The two-level recombination center was analyzed in a previous report.[24] Such two-level defects, such as the divacancy, are known to exist in irradiated silicon. However, the previous analysis concluded that the difference between a two-level system and a single-level system was greatest when the Fermi level coincided with the upper level. It was shown, for this case, that the lifetime versus injection-level curves were only slightly nonlinear and also only slightly temperature-dependent. Although the two-level system cannot be completely ruled out at this time, it would appear more fruitful to find another explanation.

The presence of two recombination levels can also be used to explain the nonlinear injection-dependence curves at higher temperatures. It is known that many different defects exist in irradiated silicon and that the introduction rates of many are comparable.[24]

The injection dependences of the higher two temperatures are replotted in Fig. 35, as was done by Germano and Curtis.[25] The error in the curves are indicated by the vertical lines. Since the lifetimes did not vary a great deal, an attempt to fit such a curve would probably not be fruitful. However, some general observations can be made.

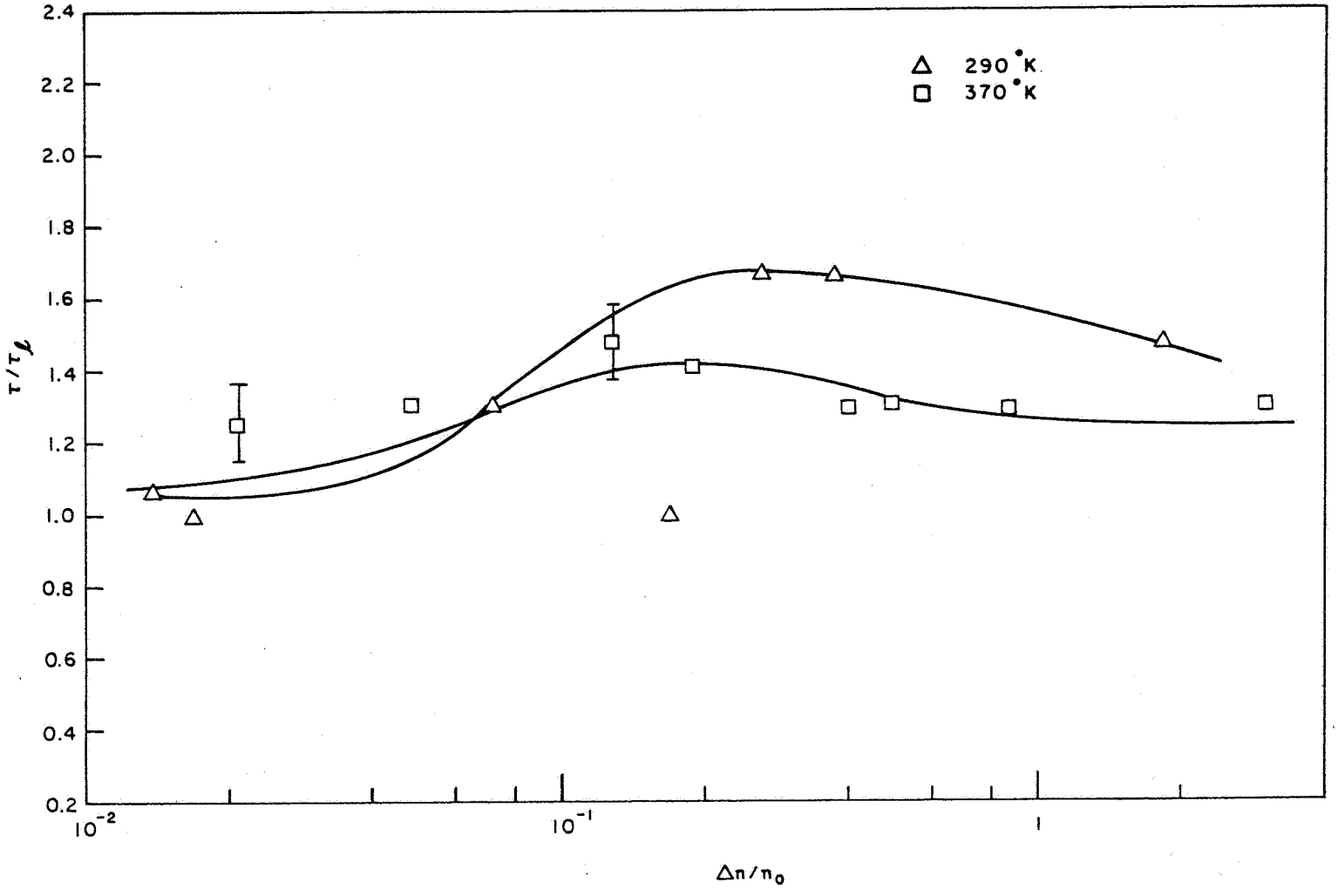

Fig. 35--Relative lifetime vs injection level for 50-ohm-cm, P-doped, FZ silicon

First, a few words should be said about the shape of the curves plotted in Fig. 35. For single levels which follow the Shockley-Read theory such that $\tau_h > \tau_\ell$, the curve for τ should start at τ_ℓ at very low values of $\Delta n/n_0$ and asymptote to τ_h at high levels equal to the order of $\Delta n/n_0 \approx 10$. At $\Delta n/n_0 = 1$, there should still be a significant rise in τ.

If for the single level $\tau_\ell > \tau_h$, then the curve for τ will start at a value of τ_ℓ at low values of $\Delta n/n_0$ and will not decrease significantly until $\Delta n/n_0 > 10^{-1}$. The minimum value for τ at $\Delta n/n_0 = 1$ for any value of τ_h/τ_ℓ is equal to $0.5\,\tau_\ell$. $\tau_\ell > \tau_h$ implies that either n_1/n_0 or p_1/n_0 in the expression for the low-level lifetime, $\tau_\ell = \tau_{p_0}(1 + n_1/n_0) + \tau_{n_0}(p_1/n_0)$, is contributing to the observed lifetime.

The curves in Fig. 35 indicate that a single-level system cannot be used in an analysis of this experimental data. Such curves are possible if a two-level system is assumed. The rise at low $\Delta n/n_0$ would be due to a level with $\tau_h/\tau_\ell > 1$ and the decrease at larger values of $\Delta n/n_0$ could be explained by the influence of the second level with $\tau_h/\tau_\ell < 1$. The observed lifetime at any value of $\Delta n/n_0$ would be $\tau = (1/\tau_1 + 1/\tau_2)^{-1}$, where τ_1 is the lifetime of level 1 and τ_2 is the lifetime of level 2. The curves of Fig. 35 also indicate that at higher injections, τ is either decreasing or staying constant. This means that either n_1/n_0 or p_1/n_0 is contributing to the observed lifetime for one of the two levels. This implies that at 290°K, $n_1/n_0 > \tau_{n_0}/\tau_{p_0}$ or that $p_1/n_0 > 1$. If $p_1/n_0 > 1$, E_R is no farther than 0.3 eV from the valence band; if $\tau_{n_0}/\tau_{p_0} \gtrsim 1$, E_R is no farther than 0.32 eV from the conduction band. Thus, E_R is no deeper than 0.32 eV for one level.

The curves of Fig. 34 for the two lower temperatures give τ_h = 0.57 μsec, τ_ℓ = 0.65 μsec for 100°K and τ_h = 4.2 μsec, τ_ℓ = 2.5 μsec for 210°K. Since $\tau_h \approx \tau_\ell$ at 100°K, n_1/n_0 or p_1/n_0 is significant in τ_ℓ. This indicates that one level is probably at least as shallow as 0.1 eV from either band. If this level, call it level 1, is still one of the two levels at 290°K, then the τ_ℓ, as measured in Fig. 33, should be due only to level 2,

since level 1 should have a very high lifetime for τ_{ℓ}. If this is true, the level seen in the QC-grown silicon can be ruled out.

It would be possible to fit the curve using the available data and assuming two recombination centers. However, such a quantitative fit requires an estimate of too many parameters, which, in view of the errors in the measurements, does not seem to be advisable at this point.

4.3.2. p-type Silicon

A 150-ohm-cm, FZ-grown, B-doped silicon sample was also irradiated with 30-MeV electrons at room temperature. The contact problem, as discussed in Section 4.1, prevented obtaining reliable measurements below about 200°K. Other experimental difficulties during the run prevented reliable measurements below about 250°K after room-temperature irradiations.

The irradiation data are presented in Fig. 36. The initial degradation rate is 5.4×10^{-8} cm^2/electrons sec. The nonlinear behavior at the higher fluences is not clear. If two different levels having different introduction rates are being introduced, there would still have been a linear behavior. A turnover, as seen, can occur if the Fermi level is moved appreciably. However, the conductivity changed only 3 percent and such a change cannot account for the observed behavior. Initially, the sample had a larger dependence of lifetime on injection level. But since the measurements were taken at low-injection levels, such an explanation is not applicable to the curve.

The temperature dependences of the carrier lifetime are shown in Fig. 37, and the injection dependences for two temperatures are shown in Fig. 38. At 360°K, this dependence is not linear. This probably indicates two levels, but with the present amount of data, the levels cannot be determined. However, it appears that one level, which dominates at $\Delta p/p_0 > 0.05$, is a level that has $\tau_h \leq \tau_{\ell}$. This means that at that temperature, the

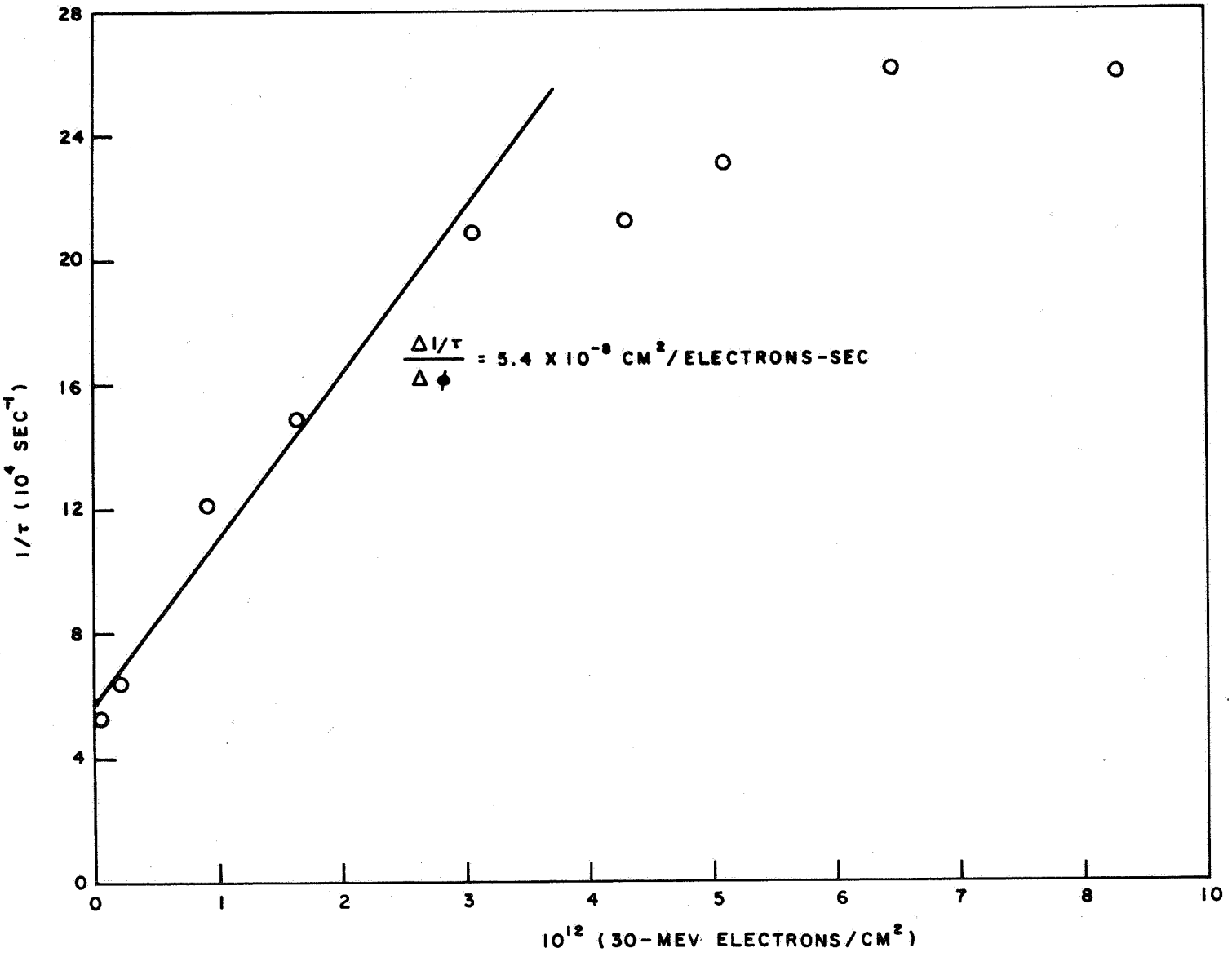

Fig. 36--Reciprocal lifetime vs integrated flux for 150-ohm-cm, B-doped, FZ silicon

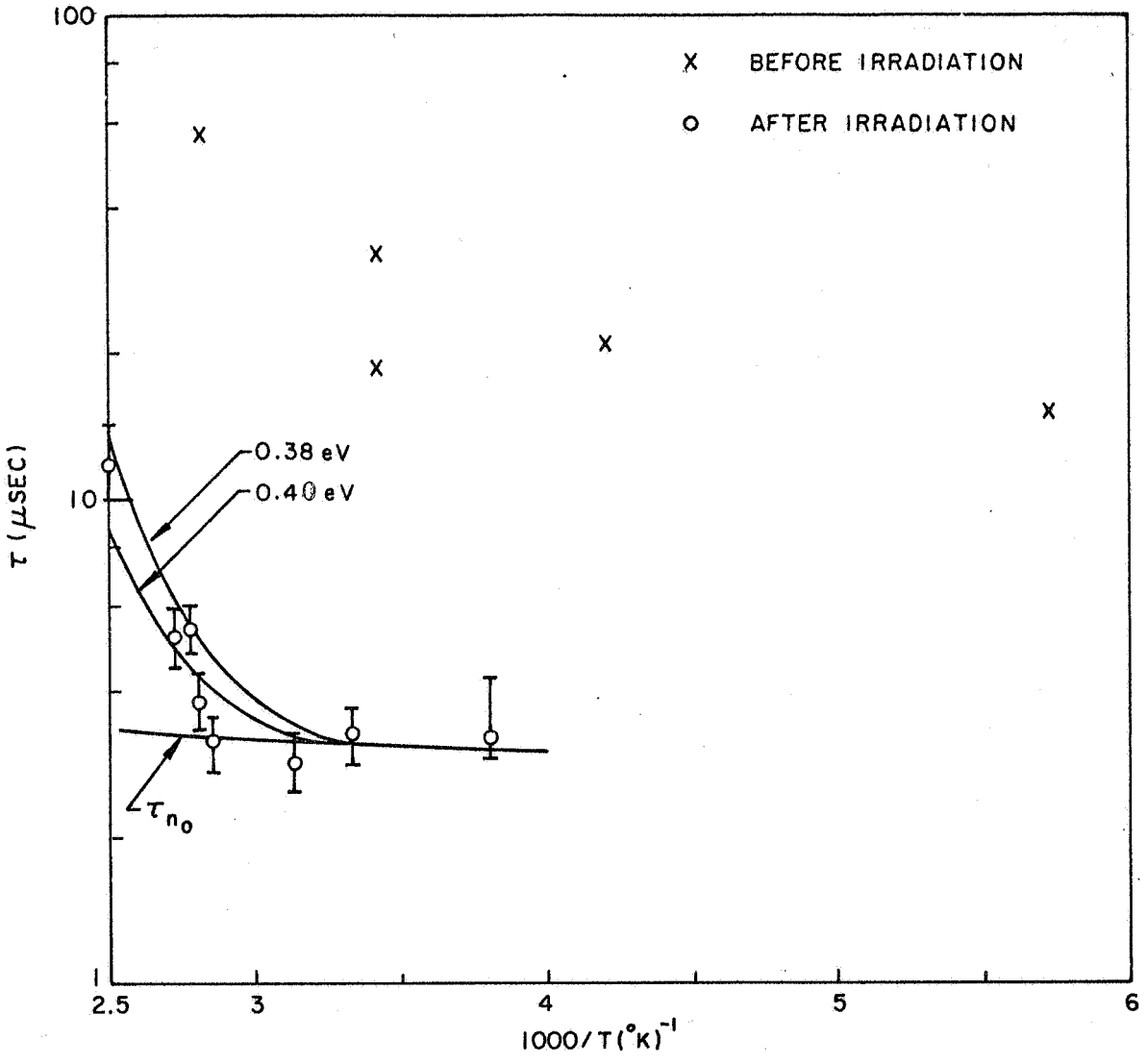

Fig. 37--Carrier lifetime vs reciprocal temperature for 150-ohm-cm, B-doped silicon

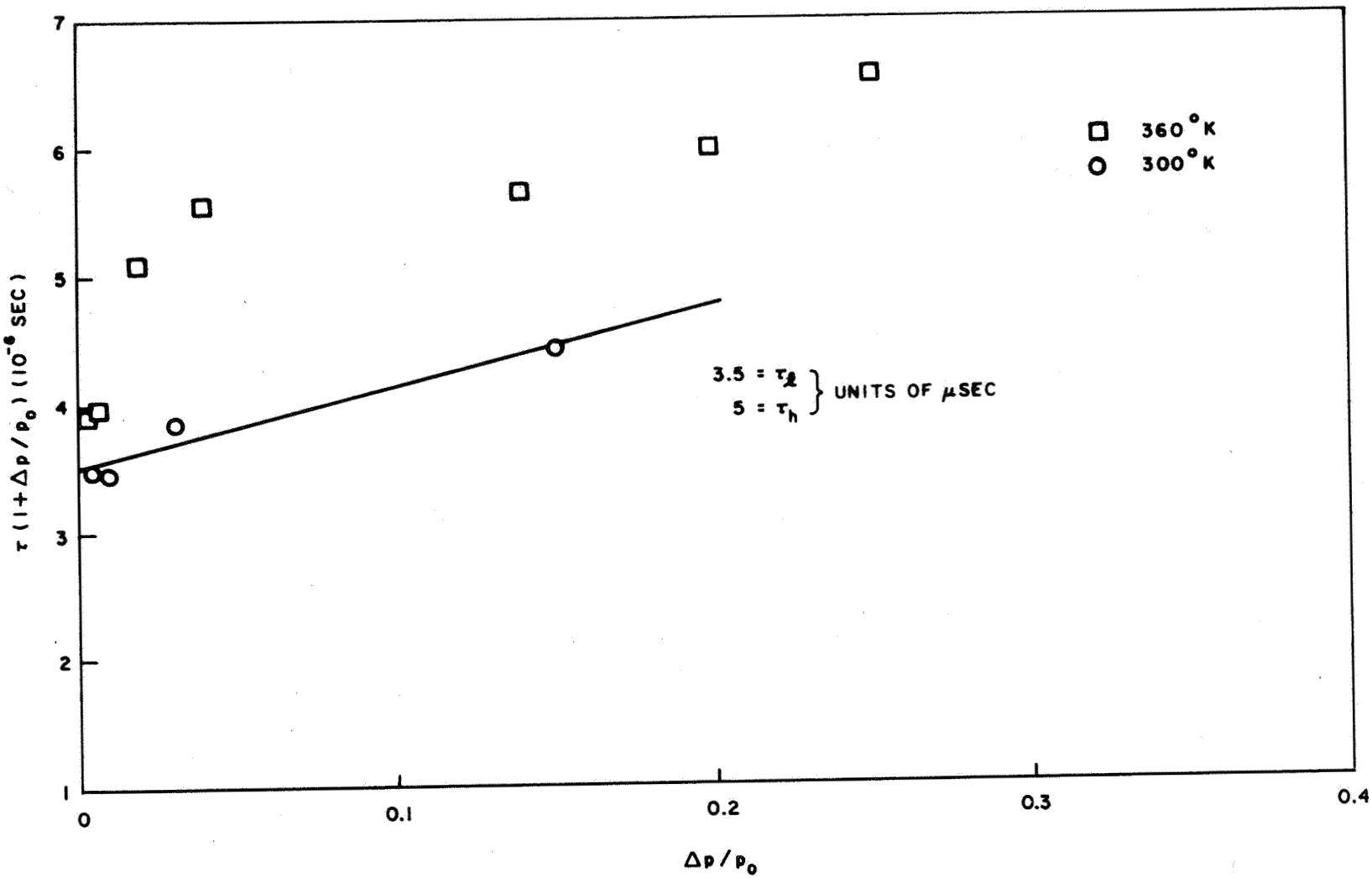

Fig. 38--Dependence of lifetime on excess carrier concentration for 150-ohm-cm, B-doped silicon

recombination level is probably closer to a band edge than to the Fermi level of the sample.

The data of Fig. 37 can be fitted to a theoretical curve for τ_ℓ. The flat portion at the lower temperature indicates that τ_{n_0} is not changing very much; this, in turn, indicates that a neutral center should be used for τ_{n_0}. The curves in Fig. 37 are based on this assumption and on the assumption of a recombination level below the center of the gap. A good fit is obtained with $E_R = 0.39$ eV. The assumption that there is a recombination level above the center of the gap cannot be discarded however.

The rather good fit to Fig. 37 probably should not be taken too seriously. The injection dependence at 360°K indicates that there are two levels at this temperature. If one level is not too temperature-dependent, then its effect on the observed lifetime should be greater at 400°K. That is, the observed lifetime is less steep than the lifetime curve for just the single level. A reasonable conclusion would be that the center causing the rise in lifetime is no greater than 0.4 eV for either band edge.

4.4. SUMMARY OF RESULTS

Three silicon samples were irradiated, and the results indicate that different centers are introduced in n-type QC-grown and in FZ-refined material. This difference is presumably due to the difference in oxygen content. The level obtained in the QC sample is an acceptor level 0.38 eV below the conduction band. This level was not seen in the FZ material. Instead, there were at least two levels, one of which is very shallow ($\sim$0.1 eV) and the other is no deeper than 0.32 eV. In the analysis of the data on the QC sample, a cross section for a neutral capture which was more temperature-dependent than given by Lax was observed. The temperature dependence of the attractive cross section was consistent with the existing theory.

In FZ p-type silicon, there was a level no greater than 0.40 eV from a band edge. The data also indicate at least two recombination centers are contributing to the observed lifetime and that one could be fitted with a neutral cross section.

V. ELECTRON-SPIN-RESONANCE STUDIES

The resonance equipment necessary for the ESR work was described in Ref. 22; it is essentially modeled after the equipment of Prof. G. Feher at the University of California, San Diego. These experiments were designed to supplement the lifetime experiments in an attempt to obtain a detailed microscopic picture of the radiation-induced recombination center responsible for the lifetime degradation. In addition, experiments have been performed on the production at 80°K of the G6 center (the divacancy in p-type silicon) and the G8 center (the vacancy-phosphorous complex in n-type silicon).

5.1. G6 CENTER

A study was made of the number of divacancies formed at 80°K by 30-MeV electrons and a comparison was made with the number formed at 300°K. The actual experiments were performed by irradiating at 80°K and then annealing the samples to 300°K. The annealing experiments were carried out in order to ascertain whether additional divacancies were formed indirectly either by the association of single mobile vacancies or by the breaking up of a vacancy complex. It was found that the introduction rate at 80°K was approximately the same as that at 300°K, namely, 0.03 cm^{-1}, and that there was at most a 10 percent increase in the number of centers even after annealing to 300°K (see Fig. 39). Thus, the number of indirectly produced divacancies is quite small, indicating that the primary interaction is the basic mechanism for producing this center. This has also been found to be true for low-energy electron irradiation.

5.2. G8 CENTER

In 0.1-ohm-cm, FZ-refined, P-doped, n-type silicon, a study of the

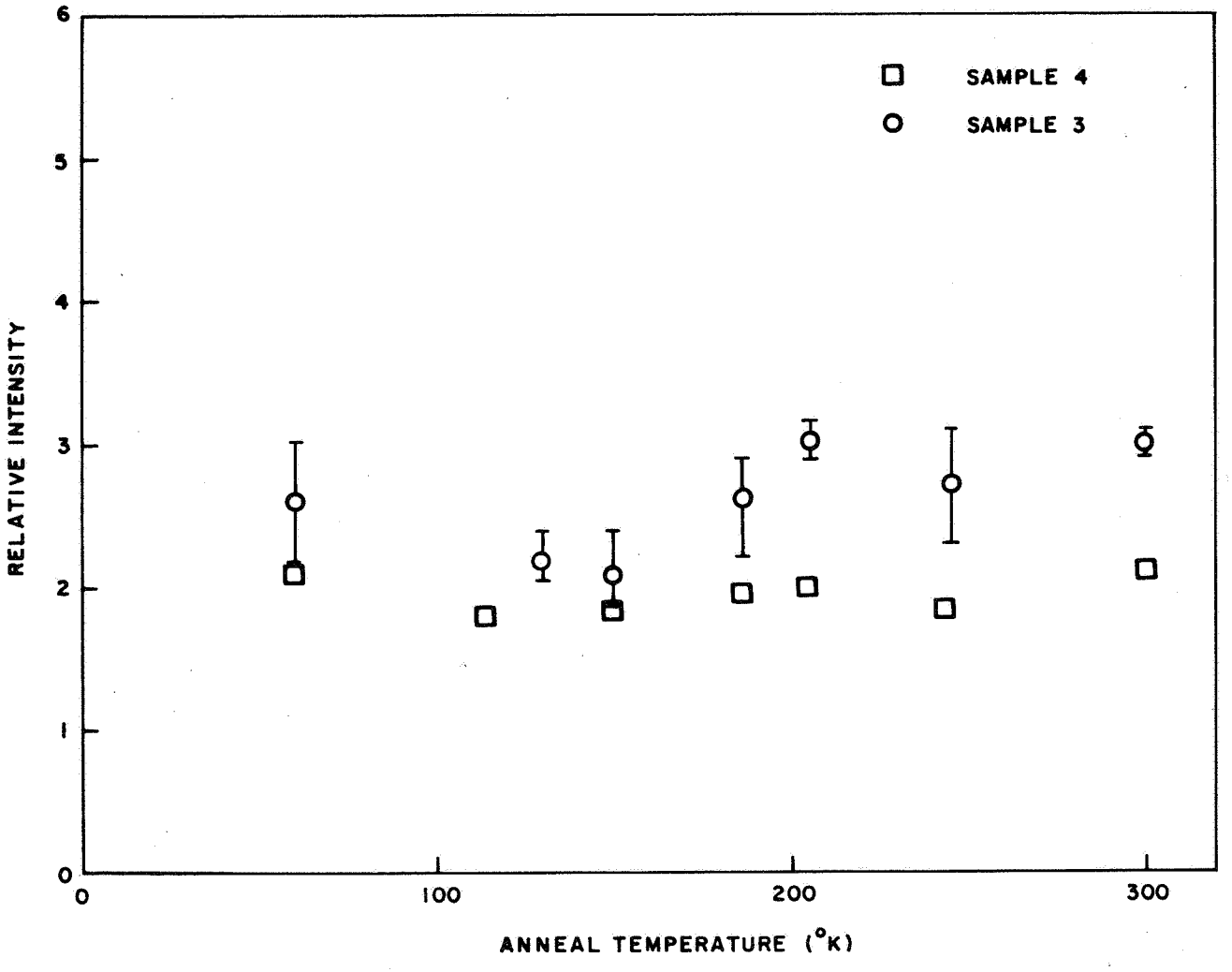

Fig. 39--Anneal of G6 center in 0.1-ohm-cm, B-doped silicon after 30-MeV electron irradiation at 80°K

number of G8 centers formed during an 80°K irradiation by 30-MeV electrons has been made for comparison with the 300°K introduction rate.* Watkins[26] found that following 1.5-MeV electron irradiations, the number of these centers increases upon annealing in the neighborhood of 120°K and 280°K. This was not observed in the current experiments; in fact, a distinctly different behavior occurred. A significant number of centers were formed at 80°K, implying that the vacancy is mobile below 80°K since the formation of this center is caused by the migration of a vacancy to the phosphorus donor. When the samples were warmed (the measurements are always made at 20°K), it was found that up to 150°K only a small change in the number of centers was observed. Further heating of the sample up to 300°K drastically reduced the number of centers until only about 10 percent of the original number remained. Coincident with this observation, the resonance associated with the divacancy (Si-G7) appears. These results are shown in Fig. 40. (A similar behavior was found for pulled material.)

For an understanding of this behavior, information on the irradiation-produced behavior is necessary. The condition stated for observation of these centers is that the Fermi level be about 0.4 eV below the conduction band.[26] In addition, as the Fermi level is still further lowered, the divacancy changes its charge state from -1 to 0 and again becomes unobservable. In order to explain the experimental observation that only the G8 center is observed with extensive radiation, it would appear that a number of deep-lying levels are formed with highly energetic radiation, i.e., 30-MeV electrons. The Fermi level is lowered by these deep levels to a position such that the divacancy is not in the correct charge state, i.e., the 0 charge state, for observation by spin resonance. Annealing rids the

*This work was supported in part under Contract DA-49-186-AMC-65(X) with Harry Diamond Laboratories, U.S. Army Materiel Command.

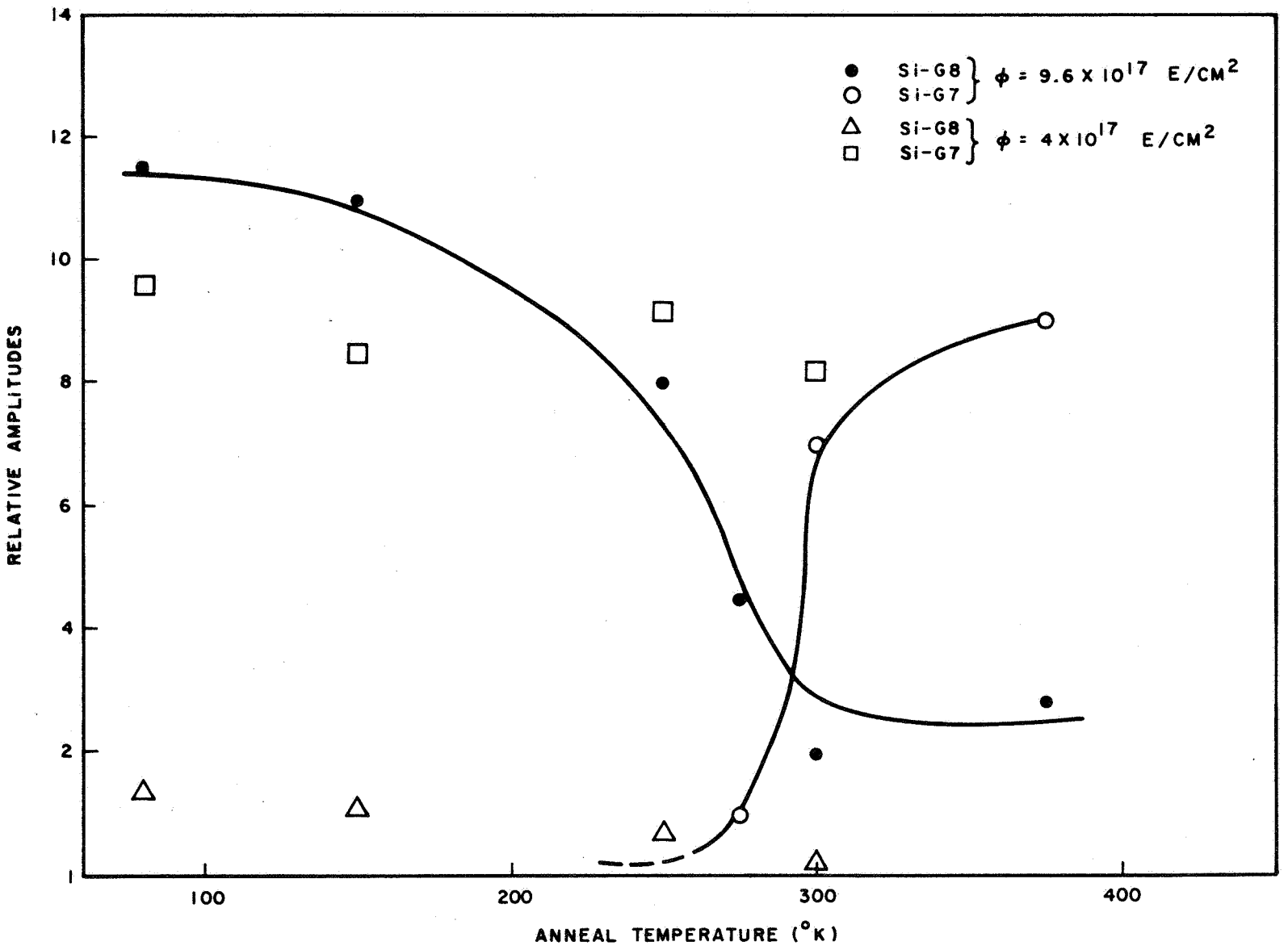

Fig. 40 --The number of Si-G7 (divacancies) centers and the number of Si-G8 (vacancy-phosphorous pairs) centers observed as a function of annealing temperature following an 80°K irradiation; results for two different amounts of total irradiation are shown

samples of the deep-lying levels and the Fermi level then rises to just above the G8 center level. Thus, that center is no longer observable with ESR, but the divacancy, whose energy level must therefore be above G8 center level, is seen. In fact, it has been found on other experiments that the Si-B1 center (0.16 eV) and the divacancy can be seen in the same sample. This means that the position of the divacancy level is ~0.16 eV below the conduction band,* instead of the previously listed value of 0.4 eV. These arguments are based on the assumption that all the observations were due to a change in the Fermi level (and hence charge state of the defects) caused by annealing of deeper levels not associated with either the G8 or G6 defect.

Two other types of experiments were made which essentially substantiate this theory. First, a number of samples were run at different flux levels. For fluxes greater than 6×10^{17} electrons/cm^2, only the G8 center was seen. For lower fluxes, the divacancy resonance was observed and in some cases a small G8 resonance, which is a factor of 5 to 10 below that for higher fluxes. Warming of the samples to 300°K produced no significant change in the intensity of the divacancy resonance, but it did produce a decrease of a factor of 2 in the number of G8 centers. Second, one of those samples in which both resonances were seen and which had been warmed to 400°K was illuminated at 20°K with a microscope lamp. The G8 center intensity had increased, the divacancy resonance had decreased, but the total number of centers remained the same. This signifies that a large number of phosphorus-vacancy complexes remain after an anneal and the decrease in the resonance intensity was actually due to a change in the electron population.

A major interest has also been to correlate the lifetime and resonance experiments. From the lifetime results, it has been observed that the energy level associated with the recombination center is about 0.38 eV below the conduction band in 50-ohm-cm, p-doped, pulled, QC material.

*Also supported in part under Contract DA-49-186-AMC-65(X).

This is possibly the Si-G16 center that has been observed in QC material, but not in FZ material, using ESR and has an energy level between 0.16 eV (the Si-B1 centers) and 0.4 eV (the G8 center). Watkins[26] indicates that this center has two energy levels, the upper of which is 0.4 eV. Our estimated introduction rate of this center, $\sim 2 \times 10^{-2}$ defects/cm, and the degradation rate constant obtained in the lifetime experiment, $\sim 4.8 \times 10^{-8}$ cm^2/sec, give a room-temperature cross section of 10^{-13} cm^2. This is a rather high cross section and would tend to rule out Si-G16 as the center seen causing the degradation in lifetime.

A direct comparison between lifetime and ESR experiments is difficult. One problem could be that if an unknown impurity with a concentration of less than 10^{14}/cm^3 governs the initial lifetime degradation, it would be impossible to see this center with resonance techniques. In resonance experiments, at least a flux of 10^{15} electrons/cm^2 is needed in order to observe known centers. Thus, for higher flux levels, centers possibly can be observed which are not correlated with the lifetime results.

It should also be mentioned that in 10-ohm-cm, P-doped samples, either QC or FZ, which have been irradiated to flux levels greater than 10^{17} electrons/cm^2, centers were seen which corresponded to those observed by Jung and Newell[27] (centers II and III) following considerable neutron irradiation. The samples were intrinsic, as expected, after irradiation. The concentration of centers being much greater than the number of phosphorous atoms and the introduction rate being comparable for the two types of material indicated a center that is independent of any known impurities in the sample. This is in agreement with the conclusion by Jung and Newell.

VI. CONCLUSIONS

From the results of lifetime studies to date on silicon using 30-MeV electrons as irradiating particles at room temperature, the following conclusions can be drawn. It is quite evident from the excess minority carrier lifetime experimental data that the defects (recombination centers) introduced in vacuum FZ-grown and Czochralski pulled, QC-grown silicon are different. There is also a difference in the recombination centers introduced in low-resistivity and high-resistivity (high-purity) silicon. Both the dc conductivity and microwave-reflection techniques measure the same property--electrical conductivity--to detect the presence of damage and to determine the characteristics of this damage in terms of minority carrier lifetime. The advantage of the microwave-reflection technique for measuring lifetimes is that it eliminates the contact problems in attaching leads to silicon and thereby facilitates obtaining reproducible measurements.

The defects that are produced in high-purity n- and p-type silicon and contribute to the degradation of carrier lifetime are recombination centers lying very near the center of the gap. In both n- and p-type materials, these defects are attractive to minority carriers; in n-type material they are within 0.05 eV of the center of the gap and in p-type material they are within 0.10 eV of the center of the gap.

A recombination level at E_c - 0.38 ±0.01 eV was found in pulled n-type silicon (50 ohm-cm), whereas two recombination levels, one very shallow (~0.1 eV) and the other no deeper than 0.32 eV from one of the band edges, were observed in FZ n-type silicon (50 ohm-cm). Furthermore, a recombination level no greater than 0.4 eV from one of the band edges was observed in FZ p-type silicon (150 ohm-cm).

Using comparison arguments, it is possible to gain some physical insight into the nature of the recombination centers introduced in silicon. The E_c - 0.38 eV level seen in n-type QC material is probably oxygen-dependent, since the only difference in this material and FZ material is presumably the oxygen content. This follows from current and past observations that the degradation constant for the two materials appears to be equal, and this would indicate that this center is not being produced at a comparable rate in FZ material.

The high-resistivity n-type silicon, which has a low oxygen content, has a recombination center very near the center of the gap. Since the radiation-induced recombination centers in 50-ohm-cm FZ n-type silicon are not seen in the high-resistivity n-type silicon and since the degradation constant for the 50-ohm-cm samples is higher than that for the high-resistivity silicon, the centers being produced in the 50-ohm-cm sample are not being produced at a comparable rate in the high-resistivity sample, because otherwise they should be seen in the high-resistivity silicon. This leads to the conclusion that the recombination centers seen in the 50-ohm-cm samples are impurity-dependent. The growth techniques of the high-resistivity samples make it impossible to know what impurities may be present in this silicon. Therefore, it is not possible to say that the recombination center defects seen in the high-resistivity silicon are unequivocally intrinsic, but may be considered reasonably so. Intrinsic is used in the sense that the defects are impurity independent, but the defect or defect configurations may require thermal motion to be produced.

In comparing the 150-ohm-cm p-type FZ silicon and the high-resistivity p-type silicon, it is possible to conclude, using the same arguments as those for n-type silicon, that the recombination centers in the 150-ohm-cm silicon are impurity-dependent, whereas the recombination centers in the high-resistivity silicon are possibly intrinsic defects. If the centers observed in the high-purity n- and p-type silicon are intrinsic, then they could be either two intrinsic centers or different charge states of the same center.

At the present time, it is not possible to definitely correlate the radiation-induced recombination centers with the damage centers observed in the ESR studies. The center at E_c - 0.38 eV in pulled material may be the Si-G16 center identified by Watkins.[21] Our ESR results indicate that the Si-G16 contains oxygen and Watkins indicates that the Si-G16 may have two levels, the highest being about 0.4 eV from the conduction band. Both of these results are consistent with the conclusion that the Si-G16 is the recombination center observed. However, in comparing the introduction rates from electron spin resonance to those from carrier lifetime data, the observed recombination center would have to have a capture cross section of 10^{-13} cm^2. The recombination centers seen in high-resistivity silicon may be the ESR centers observed after considerable 30-MeV electron irradiation[24] and also by Jung and Newell[27] following neutron irradiation. These centers (II, III), designated Si-P3,[21] were described by Jung and Newell as being impurity independent and deep in the forbidden gap.

In addition, the ESR work done under this contract has led to the following conclusions. After an irradiation of p-type silicon at 80°K, no additional divacancies are formed when the samples are annealed to 300°K. This indicates that the number of indirectly produced vacancies is quite small. In n-type silicon, a number of deep-lying defect levels, greater than 0.4 eV below the conduction band, are formed which anneal between 80°K and 300°K. In addition, it was found that the vacancy is mobile below 80°K since a significant number of Si-G8 centers are formed during an 80°K irradiation and that the formation of these centers is caused by the migration of the vacancy to the phosphorus. For the divacancy in n-type silicon, it was found that the upper energy level associated with it is above that of the Si-G8 level and indeed appears to be at most 0.16 eV from the conduction band.

REFERENCES

1. Corbett, J. W., Electron Radiation Damage in Semiconductors and Metals, Academic Press, 1966, p. 83.

2. van Lint, V. A. J., and D. P. Snowden, Radiation Effects on Silicon, Contract NAS7-289, General Atomic Division, General Dynamics Corporation, Report GA-6556, July 21, 1965.

3. Baicker, J. A., Phys. Rev., Vol. 129, 1963, p. 1174.

4. Lax, M., Phys. Rev., Vol. 119, 1960, p. 1502.

5. Shockley, W., and W. T. Read, Jr., Phys. Rev., Vol. 87, 1952, p. 835.

6. Hall, R. N., Phys. Rev., Vol. 87, 1952, p. 87.

7. Streetman, B. G., J. Appl. Phys., Vol. 37, 1966, pp. 3137, 3145.

8. Nomura, K. C., and J. S. Blakemore, Phys. Rev., Vol. 112, 1958, p. 1607.

9. _____, Phys. Rev., Vol. 121, 1961, p. 734.

10. Esposito, R. M., J. J. Loferski, and H. Flicker, J. Appl. Phys., Vol. 38, 1967, p. 825.

11. Fan, H. Y., Solid State Physics, Vol. 1, Academic Press, 1955, p. 352.

12. Champlin, K. S., D. B. Armstrong, and P. O. Gunderson, Proc. IEEE, Vol. 52, 1964, p. 677.

13. Rao, K. V., and A. Smakula, J. Appl. Phys., Vol. 37, 1966, p. 2840.

14. Champlin, K. S., and G. H. Glover, J. Appl. Phys., Vol. 37, 1966, p. 2355.

15. Sullivan, M. V., and J. H. Eigler, J. Electrochem. Soc., Vol. 103, 1956, p. 226.

16. Dunlap, W. C., Jr., An Introduction to Semiconductors, John Wiley and Sons, New York, 1957, p. 270.

17. Kittel, C., Introduction to Solid State Physics, John Wiley and Sons, New York, 1957, p. 365.

18. Ivanov, V. G., Soviet Phys.—Solid State, Vol. 8, 1966, p. 1306.

19. Jung, W., and G. S. Newell, Phys. Rev., Vol. 132, 1963, p. 648.

20. Tkuhev, V. D., A. F. Plotnikov, and V. S. Vairlov, Soviet Phys.—Solid State, Vol. 5, 1964, p. 2333.

21. Watkins, G. D., Radiation Damage in Semiconductors, Academic Press, 1964, p. 97.

22. van Lint, V. A. J., et al., Radiation Effects on Silicon Solar Cells, Final Report, Contract NAS7-91, General Atomic Division, General Dynamics Corporation, Report GA-3872, February 1963.

23. van Lint, V. A. J., et al., Radiation Effects on Silicon Solar Cells, Summary Report, Contract NAS7-91, General Atomic Division, General Dynamics Corporation, Report GA-4797, December 1963.

24. Wikner, E. G., et al., Transient Radiation Effects, Final Report, Contract DA-49-186-AMC-65(X), Harry Diamond Laboratories, U. S. Army Materiel Command, Report DA-49-186-AMC-65(X)-1, February 1967.

25. Germano, C. A., and O. L. Curtis, Jr., IEEE Trans. Nuclear Science, Vol. 13, No. 6, December 1966, p. 47.

26. Watkins, G. D., and J. W. Corbett, Discussions of the Faraday Society, No. 31, 1961, p. 86.

27. Jung, W., and G. S. Newell, Phys. Rev., Vol. 132, 1963, p. 648.